Stability of Caribbean coral communities quantified by long-term monitoring and autoregression models

Kevin Gross[1] and Peter J. Edmunds[2]

[1]Biomathematics Program, North Carolina State University, Raleigh NC 27695, USA.

[2]Department of Biology, California State University, Northridge, CA 91330, USA.

[1]Contact information of corresponding author:

email: kevin_gross@ncsu.edu

Phone: 1.919.513.8072

Fax 1.919.515.7591

Abstract

Tropical coral reefs exemplify ecosystems imperiled by environmental change. Anticipating the future of reef ecosystems requires understanding how scleractinian corals respond to the multiple environmental disturbances that threaten their survival. We analyzed the stability of coral reefs at three habitats at different depths along the south shore of St. John, US Virgin Islands, using multivariate autoregression (MAR) models and two decades of monitoring data. We quantified several measures of ecosystem stability, including the magnitude of typical stochastic fluctuations, the rate of recovery following disturbance, and the sensitivity of coral cover to hurricanes and elevated sea temperature. Our results show that, even within a ~4 km shore, coral communities in different habitats display different stability properties, and that the stability of each habitat corresponds with the habitat's known synecology. Two *Orbicella*-dominated habitats are less prone to annual stochastic fluctuations than coral communities in shallower water, but they recover slowly from disturbance, and one habitat has suffered recent losses in scleractinian cover that will not be quickly reversed. In contrast, a shallower, low-coral-cover habitat is subject to greater stochastic fluctuations, but rebounds more quickly from disturbance and is more robust to hurricanes and seawater warming. In some sense, the shallower community is more stable, although the stability arguably arises from having little coral cover left. Our results sharpen understanding of recent changes in coral communities at these habitats, provide a more detailed understanding of how these habitats may change in future environments, and illustrate how MAR models can be used to assess stability of communities founded upon long-lived species.

Keywords: autoregression, coral reefs, global climate change, hurricanes, monitoring, seawater temperature, time-series model, U.S. Virgin Islands.

Introduction

Nearly every major ecosystem on Earth has been impacted by human activity (Walther et al. 2002, Parmesan 2006). As global climate change intensifies (Stocker et al. 2013) describing and understanding these impacts will remain a primary focus of ecological science (Bellard et al. 2012) and conservation (Parmesan et al. 2013). The principle tool for describing changes in the structure and function of ecosystems is monitoring (Lindenmayer and Likens 2010), which entails the repeated measuring of demographic features or community attributes over time. Monitoring provides a foundation for describing patterns of ecosystem change, but the full value of monitoring can only be realized if it is matched by studies that illuminate the mechanisms driving change (Lovett et al. 2007, Lindenmayer and Likens 2010). Often, a mechanistic understanding of ecosystem change allows those changes to be understood within the rich conceptual framework of ecosystem stability (Holling 1973, May 1974, Ives and Carpenter 2007). In turn, the framework of ecosystem stability provides a basis for anticipating the sensitivity of ecosystems to future environmental conditions.

Tropical coral reefs support well-known, diverse, and complex communities that are renowned for their beauty and unique biology, but are also thought to be vulnerable to environmental change (Connell 1978, Nyström and Folke 2001). Over the last 30 years, ecological investigations of coral reefs have been dominated by descriptions of declining abundance of scleractinian corals (Schutte et al. 2010, Jackson et al. 2014). Although there are

a few reefs that are still dominated by scleractinians (Sandin et al. 2008), the overall prognosis for the future of coral reefs is poor (Van Hooidonk et al. 2013). Indeed, rising atmospheric CO_2 alone may imperil coral reefs through rising seawater temperature (Logan et al. 2014) and declining seawater pH (Kroeker et al. 2013). In addition, scleractinians remain vulnerable to other mortality agents including storms, disease, predators, and algal overgrowth (reviewed in Rosenberg and Loya 2004), each of which may become more severe as environmental change continues. Evaluating the capacity for coral reefs to persist despite this panoply of challenging conditions requires understanding how scleractinians respond to multiple stressors. Monitoring offers great promise for this purpose, although studies must extend over sufficiently large scales of space or time to encompass ecologically meaningful variation in environmental conditions. For example, McClanahan et al. (2007) used data from 29 sites over > 1000 km of the shores of Kenya and the Comoros Islands to resolve the effects of multiple aspects of variation in seawater temperature on coral mortality. In the present study, we use two decades of monitoring data on shallow reefs in St. John, US Virgin Islands, to assess ecosystem stability in response to multiple environmental disturbances.

As monitoring efforts have matured (Gosz et al. 2010), new methods for assessing ecosystem stability from these data have been developed (e.g., Scheffer et al. 2009, Ives and Dakos 2012). Among these, multivariate autoregression (MAR) models (Ives et al. 2003, Hampton et al. 2013) have proven particularly useful for evaluating ecosystem stability, because their parameters connect directly to several measures of stability, including temporal variance, recovery rate following a disturbance, and sensitivity to environmental covariates (Ives et al. 2003, Ives and Carpenter 2007). To date, MAR models have been most commonly

applied to communities of short-lived species, such as plankton (Hampton et al. 2013). In the present manuscript, we show how MAR models can be used to assess the effects of acute environmental stressors on coral-reef communities in the Caribbean. While our work was in progress, Cooper et al. (*in press*) simultaneously and independently developed similar MAR models to forecast the impact of future ocean warming on coral-reef communities on the Great Barrier Reef.

The shallow coral reefs of St. John provide an opportune context to explore how monitoring can be used to assess the stability of reef ecosystems. These reefs have been studied for an extended period with high spatio-temporal resolution (Rogers et al. 2008, Edmunds 2013). Moreover, like most Caribbean reefs (Gardner et al. 2003, Schutte et al. 2010), over the last 28 y these reefs have endured multiple disturbances including hurricanes (Edmunds and Witman 1991), bleaching, diseases (Miller et al. 2009), and shifts in community composition caused by the die-off of the echinoid *Diadema antillarum* (Levitan et al. 2014). Recently, Edmunds (2013) described 25 years of benthic community dynamics on the shallow reefs of St. John, and revealed how these communities have changed heterogeneously, and sometimes dramatically, in coral cover and community structure since 1987. Three nearby habitats — two *Orbicella*-dominated habitats at 9 and 14 m depth, and a near-shore habitat at 7 – 9m depth — displayed different trajectories of change over > 2 decades (Edmunds 2013). Spatially heterogeneous trajectories of changing community structure have likely contributed to the kilometer-scale variation that characterizes the reefs around both St. John and nearby St. Thomas.

The objectives of this study are to use monitoring data and MAR models to quantify several aspects of the stability of the coral reef communities in St. John, and to use this understanding to evaluate whether the community dynamics of the recent past suggest further deterioration in the future. We focus on stability properties that are related to the so-called stationary distributions of each habitat, which capture the long-run mean and variance in scleractinian coral cover (Ives et al. 2003). Using the stationary distributions, we evaluate four aspects of stability: (1) the (scaled) annual variation in coral cover, (2) the rate at which the community returns to its stationary distribution following disturbance, (3) the sensitivities of mean coral cover to hurricanes and elevated seawater temperature, and (4) the additional temporal trend in mean coral cover over two decades, after accounting for the impact of hurricanes and ocean warming. Together, these four stability properties provide a detailed understanding of how scleractinian corals in St. John are influenced by their environment, and how they are (or are not) likely to change in abundance in the future. A full description of the synecology of these reefs can be found in Edmunds (2002, 2013) and Rogers et al. (2008).

Methods

Study site and data collection

We analyzed the annual benthic community structure of three fringing-reef habitats between Cabritte Horn and White Point along ~4 km of the south shore of St. John, US Virgin Islands. Field sites and methods are described in Edmunds (2013), and are summarized here, with additional details in Appendix A. Annual monitoring in two habitats, henceforth referred to as Tektite (14 m depth) and Yawzi Point (9 m depth), has been conducted since 1987. In

both habitats, the reef consists of aggregates of *Orbicella annularis* with greater coral cover at Tektite (34% coral cover in 2012, vs. 7% at Yawzi Point in 2012; Fig. 1). In 1992, six additional sites between 7 – 9 m depth were randomly selected on hard substrata, and annual monitoring at these sites has continued since. These sites are treated as random samples of a single habitat that we refer to as the "random site" (RS) habitat. The benthic community at this RS habitat has been characterized by low (< 5%) mean coral cover for the duration of the study, although at least 17 scleractinian genera are present. Each of the three habitats was visited annually between May and August, and the benthic community structure described using photoquadrats positioned along permanently marked transects (appendix A). At all habitats, percent cover of scleractinian corals, macroalgae (generally *Halimeda*, *Lobophora*, *Padina,* and *Dictyota*), and a combined category consisting of crustose coralline algae, algal turf, and bare space (CTB) were quantified. At the RS habitat, greater photographic resolution allowed scleractinians to be separated to genus.

Cover data were averaged across photoquadrats for each habitat (or each site of the RS habitat) and year. For consistency, we analyzed data from 1992 – 2012 for all three habitats (Fig. 1). Samples were treated as evenly spaced in time, because the planar growth of corals (as detected in photoquadrats) is negligible over a few months. When calculating values for environmental covariates (see below), the interval between samples was assumed to run from August 1 of one year to July 31 of the following year.

Our analysis incorporated covariates for the effects of hurricanes and seawater temperature because these environmental conditions have strong effects on reef corals (Rogers 1993; Lesser 2011), and because they can be quantified for St. John. Hurricane activity was

quantified by classifying hurricanes as either 'major' or 'minor' based on their local impact, assigning values of 1 and 0.5 to major- and minor-impact storms, respectively, and then summing over the intervals between surveys. Seawater temperature was measured *in situ* at 9 – 14 m depth using loggers that collected data every ~ 15 min (Edmunds and Gray 2014) Temperature was averaged by day and month and converted to degree-heating months (DHMs, after Donner (2009)) using a threshold of 29.3°C (Hoegh-Guldberg 1999). DHMs were summed over the intervals between surveys.

MAR modeling

We analyzed coral reef community structure using a three-category composition consisting of scleractinians, macroalgae, and a third category of "other", which combined CTB with all other substratum cover. CTB was combined with all other cover for modeling because preliminary analyses suggested that distinguishing CTB from other cover did not improve model fit. For the RS habitat, we also completed separate analyses for the most common coral genera: *Agaricia*, *Diploria*, *Montastraea* (only *M. cavernosa*), *Orbicella*, *Porites*, and *Siderastrea* (these genera together comprised 90% of the total coral cover at the RS for these years). We refer to these analyses as the cover analysis and taxonomic analysis, respectively.

Both analyses are based on multivariate autoregressive (MAR) models, and build on the results in Ives et al. (2003) and Cooper et al. (*in press*). For the present analysis, the MAR model is

$$\mathbf{x}_t = \mathbf{a} + \mathbf{B}\mathbf{x}_{t-1} + \mathbf{C}\mathbf{u}_t + \mathbf{z}t + \mathbf{e}_t \qquad t = 2,3,\ldots . \tag{1}$$

A detailed presentation of the vectors and matrices in eq. (1) for both the cover and taxonomic analyses appears in Appendix A. For both analyses, abundances are transformed prior to modeling; transformations are described later. In the cover analysis, the vector $\mathbf{x}_t$ contains the transformed densities of cover types (e.g., coral, macroalgae, other) at time *t*, while in the taxonomic analysis, $\mathbf{x}_t$ contains the transformed densities of coral genera. The vector **a** contains regression intercepts. Each element in the matrix **B** quantifies how the abundance of one of the cover types or taxa in $\mathbf{x}_t$ affects the per capita population growth rate of either the same (diagonal elements of **B**) or a different (off-diagonal elements of **B**) component of $\mathbf{x}_t$ (Ives et al. 2003). The matrix **B** captures many of the biological processes that are important in structuring these communities, including coral-algal competition (for the cover analysis) and within-genus density-dependence (for the taxonomic analysis). The vector $\mathbf{u}_t$ contains the hurricane and sea temperature covariates, and the elements of the matrix **C** quantify how those covariates impact the per capita population growth rate of each component of $\mathbf{x}_t$. The environmental covariates in $\mathbf{u}_t$ are regarded as serially independent draws from a distribution with mean $\boldsymbol{\mu}_u$ and variance matrix $\boldsymbol{\Sigma}_u$. The term $\mathbf{z}t$ captures any (linear) time trend in the components of $\mathbf{x}_t$ after accounting for the covariates in $\mathbf{u}_t$.[1] Finally, $\mathbf{e}_t$ is a vector of serially independent random errors (independent of $\mathbf{u}_t$) drawn from a distribution with mean **0** and variance matrix $\boldsymbol{\Sigma}_e$. The $\mathbf{e}_t$ term captures fluctuations in community composition that arise from processes not explicitly

[1] We also entertained models with quadratic effects of time, but quadratic time effects never provided a statistically significant improvement in fit.

included in the model, including (for example) immigration of larval recruits and fluctuating algal herbivory.

In the typical MAR model, if the spectral radius (the magnitude of the largest eigenvalue) of **B** is < 1, then the distribution of $\mathbf{x}_t$ will approach a so-called stationary distribution that captures the long-run mean and variance of the included taxa (Ives et al. 2003, Cooper et al. *in press*). Eq. (1) doesn't permit this notion of stationarity, however, because of the term **z***t*. In lieu of a stationary distribution, we will define the quasi-stationary distribution to be the long-run probability distribution of $\mathbf{x}_t$ when the time covariate is fixed at a value t^*. Throughout, we set t^* equal to the value for 2012. We write the mean and variance of this quasi-stationary distribution as $\boldsymbol{\mu}_\mathbf{x}$ and $\boldsymbol{\Sigma}_\mathbf{x}$, respectively.[2]

As we show in Appendix B, the mean and variance of the quasi-stationary distribution of $\mathbf{x}_t$ are

$$\boldsymbol{\mu}_\mathbf{x} = \left(\mathbf{I}-\mathbf{B}\right)^{-1}\left(\mathbf{a}+\mathbf{C}\boldsymbol{\mu}_\mathbf{u}+\mathbf{z}t^*\right) \quad (2)$$

$$\mathrm{Vec}\left(\boldsymbol{\Sigma}_\mathbf{x}\right) = \left(\mathbf{I}-\mathbf{B}\otimes\mathbf{B}\right)^{-1}\mathrm{Vec}\left(\mathbf{C}\boldsymbol{\Sigma}_\mathbf{u}\mathbf{C}^T+\boldsymbol{\Sigma}_\mathbf{e}\right) \quad (3)$$

(Ives et al. 2003). In eq. (3), the Vec operator converts a matrix into a vector by stacking the columns of the matrix, and $\otimes$ is the Kronecker product. Eq. (2) – (3) show how long-run distribution of the taxa in $\mathbf{x}_t$ depend on interactions among taxa (**B**), the environment ($\boldsymbol{\mu}_\mathbf{u}$ and $\boldsymbol{\Sigma}_\mathbf{u}$), how taxa respond to the environment (**C**), and time (**z**).

[2] Note that our usage of "quasi-stationary" differs from the typical usage in stochastic-processes theory for a distribution conditioned on non-absorption at a boundary.

Eq. (2) – (3) give rise to several different measures of stability (Ives et al. 2003). First, the coefficient of variation (CV) of coral cover at the quasi-stationary distribution provides a scaled measure of annual variation in abundance that is comparable across ecosystems (May 1974). Second, the spectral radius of **B** quantifies how quickly the ecosystem returns to its quasi-stationary distribution following a disturbance (Ives et al. 2003). When the spectral radius is small, the ecosystem returns to its quasi-stationary distribution more quickly than if it is large. In contrast to the CV, the spectral radius is a property of the entire community.

We can quantify how the community's quasi-stationary distribution depends on the environment or on time by differentiating eq. (2) – (3). For example, the dependence of the mean abundance of the taxa in $\mathbf{x}_t$ on the environment or on time is given by

$$\frac{d\boldsymbol{\mu}_{\mathbf{x}}}{d\boldsymbol{\mu}_{\mathbf{u}}} = \left(\mathbf{I}-\mathbf{B}\right)^{-1}\mathbf{C}, \quad \frac{d\boldsymbol{\mu}_{\mathbf{x}}}{dt^{*}} = \left(\mathbf{I}-\mathbf{B}\right)^{-1}\mathbf{z} \ . \tag{4}$$

Similarly, the dependence of the variance of the taxa in $\mathbf{x}_t$ on the variance of the (random) environmental covariates is found by

$$\frac{d\mathrm{Vec}\left(\boldsymbol{\Sigma}_{\mathbf{x}}\right)}{d\mathrm{Vec}\left(\boldsymbol{\Sigma}_{\mathbf{u}}\right)} = \left(\mathbf{I}-\mathbf{B}\otimes\mathbf{B}\right)^{-1}\left(\mathbf{C}\otimes\mathbf{C}\right) \ . \tag{5}$$

We refer to $d\boldsymbol{\mu}_{\mathbf{x}}/d\boldsymbol{\mu}_{\mathbf{u}}$ and $d\mathrm{Vec}\left(\boldsymbol{\Sigma}_{\mathbf{x}}\right)/d\mathrm{Vec}\left(\boldsymbol{\Sigma}_{\mathbf{u}}\right)$ as "sensitivities", and to $d\boldsymbol{\mu}_{\mathbf{x}}/dt^{*}$ as the "trend". Eq. (4) – (5) capture how interactions among cover types or taxa in the reef community (as quantified in **B**) buffer the direct impacts of environment (**C**) or time (**z**) to determine the long-run community composition.

Special considerations for data from St. John

Consideration 1: Data transformations. Cover data are collected as compositions, which violate the constant variance assumption of the MAR errors. Here, we follow Cooper et al. (*in*

press) by transforming composition data to a more suitable scale using an isometric log-ratio (ilr) transformation (Egozcue and Pawlowsky-Glahn 2011; details in appendix A). A linear approximation is used to convert results back to the proportion scale for reporting. Throughout, we use the notation **x** to indicate population densities on the transformed scale, and the notation **p** to indicate population densities on the proportion scale. Because the ilr scale is based on a log transformation, and because the MAR model is linear on the transformed scale, the effects of environmental covariates on reef community composition are multiplicative on the proportion scale. Thus, we report sensitivities as the proportional change in the mean cover with respect to the environmental covariates (i.e., $d\ln\boldsymbol{\mu}_p / d\boldsymbol{\mu}_u$, or equivalently $\left(d\boldsymbol{\mu}_p / d\boldsymbol{\mu}_u\right)\times\left(1/\boldsymbol{\mu}_p\right)$, instead of $d\boldsymbol{\mu}_p / d\boldsymbol{\mu}_u$; appendix A). At the RS, summed coral cover never exceeded 10%, and thus data for coral genera were log-transformed to stabilize the variance. Prior to transformation, one-half of the smallest non-zero observation in the data set was added to each data point to accommodate years when a genus was not observed at a particular site (as occurred at 18% of all genus × year × site combinations).

Consideration 2: Data from multiple locations. For the RS data, we assume that the mean abundance of the cover types and coral genera differed across the sites, but that the interactions among taxa, the effect of the environment, and the distribution of the environmental covariates were the same across sites. Based on an exploratory data analysis, we assumed a common time trend across sites for the cover analysis, but site-specific time trends for the taxonomic analysis. Thus, the MAR model included a site-specific intercept vector **a** (and a site-specific trend vector **z** in the taxonomic analysis), but all other model

parameters were common across sites. For analysis and reporting, we averaged site-specific parameters across sites to yield a common quasi-distribution that describes a typical site.

Consideration 3: Competition among coral genera at low cover sites. Coral cover at the RS habitat is sufficiently low that coral colonies rarely encounter one another on the benthos, and thus competition among coral genera is unlikely to be important. In fact, a model with interactions among genera only provided a marginally improved fit compared to a model without those interactions ($F_{30,600}$=1.46, p=0.055; this test is approximate, because it requires an assumption that the $\mathbf{e}_t$ are normally distributed). Thus, we set the off-diagonal elements of **B** to 0 in the taxonomic model.

Parameter estimation and statistical inference

MAR model parameters were estimated with conditional least-squares (Ives et al. 2003). Standard regression diagnostics were used to evaluate the quality of the model fits and homogeneity of variance (Appendix C). To accommodate non-normality of residuals, a nonparametric bootstrap with 5000 bootstrap replicates was used for statistical inference (Ives et al. 2003). Bootstrap replicates that generated a non-stationary model (spectral radius > 1; < 0.1% of bootstrap replicates) were discarded. Bootstrap distributions for a few parameter estimates were strongly skewed, so a robust bootstrap standard error with α = 0.95 (Efron and Tibshirani 1994) was used throughout. For the RS data, residuals were re-sampled as yearly blocks to preserve any spatial correlation among the sites. We conducted a small simulation study (Appendix D) to investigate the statistical properties of our estimators.

Results

Cover at three habitats

In the estimated quasi-stationary distribution for 2012 (Fig. 2), coral cover is higher at Tektite (31.7% at the distribution's metric center [appendix A], s.e. = 4.1%) and low at both Yawzi Point (5.3%, s.e. 0.8%) and the RS (3.0%, s.e. = 0.9%). Macroalgae cover was lowest at Tektite (30.9%, s.e. = 3.8%), highest at Yawzi Point (43.1%, s.e. = 6.7%) and intermediate at the RS (32.2%, s.e. = 8.3%). At all three habitats, the center of the quasi-stationary distribution has shifted towards greater algal cover from 1992 – 2012, although the extent to which algal cover has increased at the expense of decreases in coral cover (vs. decreases in 'other') differs across the three habitats (Fig. 2).

CV of coral cover and the spectral radius quantify the stability of each habitat at the quasi-stationary distribution (Fig. 3). The estimated CV of coral cover was lowest at Tektite, intermediate at Yawzi Point, and largest at the RS (Fig. 3a). In contrast, the spectral radii at Tektite and Yawzi Point were roughly equal, but larger than the spectral radius at the RS (Fig. 3b). The estimated spectral radii suggest that communities at the RS habitats return to a pre-disturbance state more quickly than communities at either Tektite or Yawzi Point. Using conventional thresholds for statistical significance, the CV of coral cover at Tektite is significantly less than the CV of coral cover at the RS (two-tailed $p = 0.006$). No other pairwise comparison between habitats is significant at the 5% level for either CV or spectral radius. Our simulation study (Appendix D) suggested that there may be considerable bias (on the order of 20 – 30%) in the estimate of spectral radius for time series of this length. Bias of this magnitude suggests that comparisons of estimated spectral radii should be interpreted cautiously.

Sensitivities (eq. 4) of coral cover quantify how hurricanes and seawater temperature impact community composition at these habitats (Fig. 4a,b). Fig. 4a,b shows proportional sensitivities of coral cover calculated with respect to a 50% increase in hurricane impact and to a 50% increase in DHMs. For example, the proportional sensitivity of -5.5% (s.e. 2.5%) to hurricane activity for Yawzi Point suggests that a 50% increase in hurricane activity is associated with a 5.5% proportional decrease in long-term coral cover. In contrast, at Tektite the same change in hurricane activity is associated with a 0.2% decrease (s.e. 1.6%) in coral cover. Estimated annual trends (Fig. 4c) show how coral cover has changed at each habitat after accounting for the impacts of hurricanes and sea temperature. Using traditional thresholds of statistical significance, but without correcting for multiple comparisons, the following sensitivities and trends are statistically distinguishable from zero: the sensitivity of coral cover at Yawzi Point to hurricane activity ($p = 0.008$) and temperature ($p = 0.002$), and the trend in coral cover at Tektite ($p = 0.028$) and Yawzi Point ($p = 0.003$). Additionally, the trend at Yawzi Point is significantly different from the trend at Tektite ($p = 0.024$) and at the RS ($p = 0.003$). Sensitivities and trends computed for macroalgae (appendix E) suggest that seawater warming will increase macroalgal cover at all three habitats, while hurricane activity will have a more pronounced impact on macroalgal cover at Yawzi Point than at either Tektite or the RS habitat. Sensitivities of the variance in coral cover (eq. 5) suggest that variability in hurricanes and seawater temperature has a greater impact on annual variability in coral cover at Yawzi Point than at the other two habitats (appendix E), although the statistical uncertainty in these sensitivities is large.

317 *Coral genera at the RS habitat*

318 Quasi-stationary distributions for the 6 common coral genera in the RS were strongly
319 right-skewed (Fig. 5). The strong skew of the quasi-stationary distribution suggests that these
320 genera will occasionally occur at relatively high abundance, but will be relatively scarcer during
321 the majority of years and at the majority of sites. The genus with the greatest predicted
322 abundance is *Porites*, which is predicted to cover 1.31% (s.e. = 0.14%) of the benthos under
323 stationary conditions, which equates to 42% of the total cover of these six most common
324 genera at the RS.

325 Estimated sensitivities of coral genera suggest that *Agaricia* is sensitive to both
326 hurricanes (Fig. 6a; $p = 0.018$) and seawater temperature (Fig. 6b; $p < 0.001$). None of the other
327 genera show statistically significant sensitivities to either environmental covariate at the RS
328 habitat. After accounting for hurricanes and sea temperature, *Diploria* (+6.8% y^{-1}, s.e. 1.8%, $p <$
329 0.001) and *Porites* (+7.0% y^{-1}, s.e. 0.6%, $p < 0.001$) show evidence of increasing cover over the
330 duration of this study (Fig. 6c). While these two rates are comparable, they reflect different
331 patterns of growth, as *Diploria* has increased from near absence in 1992 to low abundance in
332 2012, while *Porites* has increased from moderate to (relatively) high abundance (Fig. 5). None
333 of the other genera showed a statistically significant trend over time.

334 Estimates and robust bootstrap standard errors of MAR model parameters are
335 presented in Appendix E.

336

337 **Discussion**

Anticipating the responses of ecosystems to future environmental change is one of the preeminent challenges facing contemporary ecology. On tropical coral reefs, large recent declines in coral abundance together with a multitude of environmental threats to scleractinian fitness have led to gloomy forecasts for the fate of reefs (Hoegh-Guldberg et al. 2007, Van Hooidonk et al. 2013). Nevertheless, our understanding of how coral reef communities respond to environmental change is still spatially, temporally, and taxonomically coarse. Resolving how scleractinians are impacted by separate environmental stressors is necessary to acquire a deeper understanding the natural variation in coral dynamics on reefs. Here, we analyzed two decades of dynamics of coral reef communities in St. John to obtain a more detailed understanding of how these communities respond to environmental change. The four stability metrics that we calculated provide both a sharper retrospective understanding of the drivers of recent community shifts, and enable predictions of how these communities may continue to change in the near future. Further, we suggest below that the stability of these communities can be connected to their known synecology, as it has been described elsewhere (e.g., Edmunds 2002, 2013, Rogers et al. 2008). This connection to the processes that govern community dynamics, structure and composition is important because it emphasizes that stability is an emergent property of those processes. In turn, this mechanistic understanding suggests how this study of corals in St. John may enlighten the study of other coral communities with similar structure and taxa.

In the *Orbicella*-dominated habitats at Tektite and Yawzi Point, as elsewhere in the Caribbean (Jackson et al. 2014), coral cover has declined in recent decades, and macroalgal cover has increased concomitantly. Our estimate of the quasi-stationary distribution (depicted

by the approximate probability contours in Fig. 2) suggests that these shifts in community composition are not merely random walks resulting from typical annual stochastic fluctuations, but instead are evidence that the communities have responded in a directional manner to sustained alterations of their environment. Although both Tektite and Yawzi Point habitats exhibit qualitatively similar trends in cover composition, the magnitude of those trends differs, with more severe coral-cover decline at Yawzi Point. The CV and spectral radii of the Tektite and Yawzi Point habitats are also similar (Fig. 3), suggesting that both habitats ultimately display similar variability (after adjusting for the several-fold differences in recent coral cover) and recovery rates from disturbance. The immediate impacts of these disturbances may be very different, however. Sensitivity calculations suggest that corals at Yawzi Point are vulnerable to hurricanes, while corals at Tektite are considerably less afflicted by these storms (Fig. 4a). This difference is likely related to the protection from damaging storm waves provided by Tektite's greater depth and position in the lee of Cabritte Horn (Edmunds and Witman 1991, Edmunds 2013). Seawater warming also reduced coral cover at Yawzi Point (Fig. 4b), but had a more mild (and statistically insignificant) impact on coral cover at Tektite.

The less severe effect of temperature on coral at Tektite is not consistent with a previous report of bleaching, coral disease, and a striking decline in coral cover at Tektite in 2005 in the wake of an unusually warm summer (Miller et al. 2009). While we observed a modest (17%) decline in coral cover at Tektite from 2005-06, we observed a more severe (30%) decline the following year, when seas were cooler (but still eclipsed the 29.3 °C bleaching threshold). The difference between our findings and those of Miller et al. (2009) may illustrate heterogeneous responses to seawater warming over spatial scales as small as hundreds of

meters. Or, it may also suggest that the full impact of thermal stress on coral health may take multiple years to manifest as reduced cover. Delayed impacts of thermal stress could be generated by the slow onset of disease, by mortality that accrues only after consecutive years of compromised coral performance (Knowlton et al. 1990), or by the splitting of large colonies into small ones that subsequently experience greater mortality (Hernández-Pacheco et al. 2011). If delayed impacts of disturbance are important, then the full impact of variation in seawater temperature on coral cover may be greater than our results suggest, because the MAR model (at least with a single time lag) only captures the immediate (i.e., same-year) impacts of environmental disturbances. Although beyond the scope of the present study, MAR models with multiple time lags may provide a profitable avenue for exploring this possibility.

Delayed impacts of disturbance may also contribute to the additional decrease in coral cover found at both Tektite and Yawzi Point after accounting for the immediate impacts of hurricanes and seawater warming (Fig. 4c). Other factors that might have contributed to this additional coral loss include declining seawater pH (Gledhill et al. 2008), low post-settlement success of coral recruits (Arnold et al. 2010), and dynamic feedback in which decreases in reef structural complexity reduce algal herbivory (Mumby et al. 2007).

The stability of the low-coral cover communities at the RS habitat differs from Tektite and Yawzi Point. When scaled relative to abundance, annual coral cover at the RS is highly variable, both for all scleractinians (Fig. 3a), and for individual genera (Fig. 5). The spectral radius of the RS suggests that this habitat recovers quickly from disturbance, although differences in spectral radii among the three habitats are not statistically significant (Fig. 3b). Coral cover at the RS habitat appears somewhat vulnerable to ocean warming, but relatively

404 robust to hurricanes, and (unlike corals at Tektite or Yawzi Point) shows no evidence of an
405 additional temporal trend in abundance (Fig. 4). Taken together, these stability properties are
406 consistent with our previous interpretation (Edmunds 2013) that the RS habitat is characterized
407 by rapid population turnover of scleractinians, regular replenishment of coral populations
408 through external larval recruitment, and a relative insensitivity to environmental factors
409 threatening coral reefs.

410 With respect to the coral genera at the RS habitat, our results support the suggestion
411 that the eurytopic genus *Porites* will proliferate on benthic communities on shallow reefs in the
412 Caribbean in near future (Burman et al. 2012, Darling et al. 2012, Edmunds 2013). *Porites* is
413 both the most abundant genus in the quasi-stationary distribution (Fig. 5), and it has shown the
414 strongest increasing trend in coral cover (Fig. 6). In contrast to *Porites*, *Agaricia* appears
415 susceptible to hurricanes and seawater warming (Fig. 6). This finding corroborates suggestions
416 that *Agaricia* will be rarer in future communities because of its high susceptibility to thermal
417 stress (Aronson et al. 2000, Smith et al. 2013). All other common genera at the RS habitat
418 appear relatively robust to hurricanes and seawater warming, although the low mean cover of
419 some genera (notably *Montastrea*) likely compromised statistical power to detect modest
420 sensitivities here. Together, the taxonomic results reinforce the notion that responses of
421 scleractinians to environmental conditions will vary predictably among coral genera, suggesting
422 that future reef communities will consist of assemblages with a greater proportion of "winning"
423 taxa and fewer "losing" taxa (Loya et al. 2001, Darling et al. 2012, Edmunds et al. 2014).

424 What do the results of this analysis portend for coral communities in St. John in the near
425 future, if environments become even harsher? Our analysis shows that the stability of these

communities is nuanced, and suggests heterogeneous responses to environmental change even within ~4 km of shore. At Tektite and Yawzi Point, lower (scaled) annual variation in coral cover is coupled with slower recovery from disturbance. This finding is consistent with the expectation of slow population dynamics for long-lived, sporadically recruiting taxa such as *Orbicella* spp. vs. more rapid dynamics for the short-lived, rapidly recruiting corals (i.e., "weedy" taxa) of the RS habitat. However, sensitivities suggest that corals at Yawzi Point (already considerably more scarce than 25y ago) are vulnerable to additional coral loss if hurricanes become more frequent or seas become warmer. Trend statistics also suggest that corals at Tektite and Yawzi Point have experienced chronic losses that cannot be attributed to the immediate impacts of hurricanes and warming. Without a mechanistic explanation for these trends, it is difficult to suggest whether they may continue in future years. However, the slow dynamics already revealed in these habitats suggest that additional coral losses will require multiple years of less disturbed conditions if these communities are to recover their abundance of twenty-five years ago.

Coral at the RS habitats, on the other hand, may exhibit highly variable cover across time and space, but always cover only a small fraction of the benthos. These coral communities quickly recover from disturbance, and with the possible exception of *Agaricia* spp., appear relatively robust to further change by environmental stressors. The quick recovery and relative insensitivity to environmental stress of the coral communities in the RS habitat suggest that, while some coral genera (e.g., *Porites)* may increase in abundance and others (*Agaricia*) may decline in coming years, the aggregate coral cover and benthic community of the near future is likely to be fairly similar to that of the recent past. This stasis suggests stability, but by and

448 large it is a stability borne of coral rarity. That is, one interpretation of the present results is
449 that the stability of the RS habitat is a consequence of their low coral cover and the absence of
450 larger, longer-lived, more structurally complex coral colonies like those of *Orbicella*. Thus, while
451 the stability of the RS habitat is a real property of these communities, it could also indicate a
452 degraded ecosystem with little left to lose.

453 We close with a methodological comment. MAR models require time series of
454 considerable duration to yield precise and unbiased estimates of stability. In the present
455 analysis, two decades of data provide enough statistical power to identify the largest effects.
456 However, smaller environmental effects (e.g., sensitivity of coral to sea temperature at Tektite),
457 and more subtle differences in stability between ecosystems must be viewed with caution
458 when they fail to meet conventional standards of statistical significance, or (in the case of
459 spectral radii) may be estimated with considerable bias. As a practical matter, the broader
460 adoption of MAR models to estimate stability from monitoring data would be facilitated by a
461 deeper understanding of the small-sample statistical properties of these models, including
462 power and bias. Evaluating the properties of statistical estimators in MAR models will be
463 complicated, and will depend on a multitude of factors, including the number of taxa, the
464 generation time of those taxa, the number of environmental covariates, and pre-existing
465 biological knowledge that can be used to structure the matrices **B** or **C**. Yet, even a rough
466 understanding of the relationship between data duration and the properties of its statistical
467 estimators would be a welcome advance, and could inform both the design and continuation of
468 monitoring studies, and strategic decisions at the time of analysis.
469

Acknowledgments

The data analyzed in this article would not have been collected without the support of many field assistants, dedicated shore-side staff, and funding from numerous sources, including most recently the NSF LTREB program (DEB 03-43570, 08-41441 and 13-50146). This project was catalyzed by the NCEAS (NSF grant EF-0553768) working group "Tropical coral reefs of the future". We thank M. Spencer, J. F. Bruno, and two anonymous reviewers for thoughtful discussion and comments about the manuscript.

Literature cited

Arnold, S. N., R. S. Steneck, and P. J. Mumby. 2010. Running the gauntlet: inhibitory effects of algal turfs on the processes of coral recruitment. Marine Ecology Progress Series 414:91–105.

Aronson, R. B., W. F. Precht, I. G. Macintyre, and T. J. T. Murdoch. 2000. Ecosystems: Coral bleach-out in Belize. Nature 405:36.

Bellard, C., C. Bertelsmeier, P. Leadley, W. Thuiller, and F. Courchamp. 2012. Impacts of climate change on the future of biodiversity. Ecology Letters 15:365–377.

Burman, S. G., R. B. Aronson, and R. van Woesik. 2012. Biotic homogenization of coral assemblages along the Florida reef tract. Marine Ecology Progress Series 467:89–96.

Connell, J. H. 1978. Diversity in tropical rain forests and coral reefs.

489 Cooper, J.K., M. Spencer, and J. F. Bruno. Stochastic dynamics of a warmer Great Barrier Reef.
490 Ecology, *in press.*

491 Darling, E. S., L. Alvarez-Filip, T. A. Oliver, T. R. McClanahan, and I. M. Côté. 2012. Evaluating
492 life-history strategies of reef corals from species traits. Ecology Letters 15:1378–1386.

493 Donner, S. D. 2009. Coping with commitment: projected thermal stress on coral reefs under
494 different future scenarios. PLoS One 4:e5712.

495 Edmunds, P. J. 2002. Long-term dynamics of coral reefs in St. John, US Virgin Islands. Coral
496 Reefs 21:357–367.

497 Edmunds, P. J. 2013. Decadal-scale changes in the community structure of coral reefs of St.
498 John, US Virgin Islands. Marine Ecology Progress Series 489:107–123.

499 Edmunds, P. J., M. Adjeroud, M. L. Baskett, I. B. Baums, A. F. Budd, R. C. Carpenter, N. S. Fabina,
500 T.-Y. Fan, E. C. Franklin, K. Gross, X. Han, L. Jacobson, J. S. Klaus, T. R. McClanahan, J. K.
501 O'Leary, M. J. H. van Oppen, X. Pochon, H. Putnam, T. B. Smith, M. Stat, H. Sweatman, R.
502 van Woesik, and R. D. Gates. 2014. Persistence and change in community composition of
503 reef corals through present, past, and future climates. PLoS One in press.

504 Edmunds, P. J., and S. C. Gray. 2014. The effects of storms, heavy rain, and sedimentation on
505 the shallow coral reefs of St. John, US Virgin Islands. Hydrobiologia:1–16.

506 Edmunds, P. J., and J. D. Witman. 1991. Effect of Hurricane Hugo on the primary framework of a
507 reef along the south shore of St. John, US Virgin Islands. Marine Ecology Progress Series
508 78:201–204.

509 Efron, B., and R. J. Tibshirani. 1994. An introduction to the bootstrap. CRC press.

510 Egozcue, J. J., and V. Pawlowsky-Glahn. 2011. Basic concepts and procedures. Pages 12–28 *in* V.
511 Pawlowsky-Glahn and A. Buccianti, editors. Compositional data analysis: theory and
512 applications. John Wiley and Sons New York, NY.

513 Egozcue, J. J., V. Pawlowsky-Glahn, G. Mateu-Figueras, and C. Barcelo-Vidal. 2003. Isometric
514 logratio transformations for compositional data analysis. Mathematical Geology 35:279–
515 300.

516 Gardner, T. A., I. M. Côté, J. A. Gill, A. Grant, and A. R. Watkinson. 2003. Long-term region-wide
517 declines in Caribbean corals. Science 301:958–960.

518 Gledhill, D. K., R. Wanninkhof, F. J. Millero, and M. Eakin. 2008. Ocean acidification of the
519 greater Caribbean region 1996--2006. Journal of Geophysical Research 113.

520 Gosz, J. R., R. B. Waide, and J. J. Magnuson. 2010. Twenty-eight years of the US-LTER program:
521 experience, results, and research questions. Pages 59–74 Long-Term Ecological Research.
522 Springer.

523 Hampton, S. E., E. E. Holmes, L. P. Scheef, M. D. Scheuerell, S. L. Katz, D. E. Pendleton, and E. J.
524 Ward. 2013. Quantifying effects of abiotic and biotic drivers on community dynamics with
525 multivariate autoregressive (MAR) models. Ecology 94:2663–2669.

526 Hernández-Pacheco, R., E. A. Hernández-Delgado, and A. M. Sabat. 2011. Demographics of
527 bleaching in a major Caribbean reef-building coral: Montastraea annularis. Ecosphere
528 2:art9.

529 Hoegh-Guldberg, O. 1999. Climate change, coral bleaching and the future of the world's coral
530 reefs. Marine and Freshwater Research 50:839–866.

531 Hoegh-Guldberg, O., P. J. Mumby, A. J. Hooten, R. S. Steneck, P. Greenfield, E. Gomez, C. D.
532 Harvell, P. F. Sale, A. J. Edwards, K. Caldeira, and others. 2007. Coral reefs under rapid
533 climate change and ocean acidification. Science 318:1737–1742.

534 Holling, C. S. 1973. Resilience and stability of ecological systems. Annual Review of Ecology and
535 Systematics:1–23.

536 Van Hooidonk, R., J. A. Maynard, and S. Planes. 2013. Temporary refugia for coral reefs in a
537 warming world. Nature Climate Change 3:508–511.

538 Ives, A. R., and S. R. Carpenter. 2007. Stability and diversity of ecosystems. Science 317:58–62.

539 Ives, A. R., and V. Dakos. 2012. Detecting dynamical changes in nonlinear time series using
540 locally linear state-space models. Ecosphere 3:art58.

541 Ives, A. R., B. D. Dennis, K. L. Cottingham, and S. R. Carpenter. 2003. Estimating community
542 stability and ecological interactions from time-series data. Ecological Monographs 73:301–
543 330.

544 Jackson, J. B. C., M. K. Donovan, K. L. Cramer, and V. V Lam. 2014. Status and Trends of
545 Caribbean Coral Reefs. Global Coral Reef Monitoring Network, IUCN, Gland, Switzerland.

546 Knowlton, N., J. C. Lang, and B. D. Keller. 1990. Case study of natural population collapse: post-
547 hurricane predation on Jamaican staghorn corals.

548 Kroeker, K. J., R. L. Kordas, R. Crim, I. E. Hendriks, L. Ramajo, G. S. Singh, C. M. Duarte, and J.-P.
549 Gattuso. 2013. Impacts of ocean acidification on marine organisms: quantifying
550 sensitivities and interaction with warming. Global Change Biology 19:1884–1896.

551 Levitan, D. R., P. J. Edmunds, and K. E. Levitan. 2014. What makes a species common? No
552 evidence of density-dependent recruitment or mortality of the sea urchin Diadema
553 antillarum after the 1983--1984 mass mortality. Oecologia:1–12.

554 Lindenmayer, D. B., and G. E. Likens. 2010. The science and application of ecological
555 monitoring. Biological Conservation 143:1317–1328.

556 Logan, C. A., J. P. Dunne, C. M. Eakin, and S. D. Donner. 2014. Incorporating adaptive responses
557 into future projections of coral bleaching. Global change biology 20:125–139.

558 Lovett, G. M., D. A. Burns, C. T. Driscoll, J. C. Jenkins, M. J. Mitchell, L. Rustad, J. B. Shanley, G. E.
559 Likens, and R. Haeuber. 2007. Who needs environmental monitoring? Frontiers in Ecology
560 and the Environment 5:253–260.

561 Loya, Y., K. Sakai, K. Yamazato, Y. Nakano, H. Sambali, and R. Van Woesik. 2001. Coral bleaching:
562 the winners and the losers. Ecology Letters 4:122–131.

563 May, R. M. 1974. Stability and complexity in modely ecosystems. Princeton University Press,
564 Princeton, NJ, USA.

565 McClanahan, T. R., M. Ateweberhan, C. A. Muhando, J. Maina, and M. S. Mohammed. 2007.
566 Effects of climate and seawater temperature variation on coral bleaching and mortality.
567 Ecological Monographs 77:503–525.

568 Miller, J., E. Muller, C. Rogers, R. Waara, A. Atkinson, K. R. T. Whelan, M. Patterson, and B.
569 Witcher. 2009. Coral disease following massive bleaching in 2005 causes 60% decline in
570 coral cover on reefs in the US Virgin Islands. Coral Reefs 28:925–937.

571 Mumby, P. J., A. Hastings, and H. J. Edwards. 2007. Thresholds and the resilience of Caribbean
572 coral reefs. Nature 450:98–101.

573 Nyström, M., and C. Folke. 2001. Spatial resilience of coral reefs. Ecosystems 4:406–417.

574 Parmesan, C. 2006. Ecological and Evolutionary Responses to Recent Climate Change. Annual
575 Review of Ecology, Evolution, and Systematics 37:637–669.

576 Parmesan, C., M. T. Burrows, C. M. Duarte, E. S. Poloczanska, A. J. Richardson, D. S. Schoeman,
577 and M. C. Singer. 2013. Beyond climate change attribution in conservation and ecological
578 research. Ecology Letters 16:58–71.

579 Rogers, C. S., J. Miller, E. M. Muller, P. Edmunds, R. S. Nemeth, J. P. Beets, A. M. Friedlander, T.
580 B. Smith, R. Boulon, C. F. G. Jeffrey, and others. 2008. Ecology of coral reefs in the US
581 Virgin Islands. Pages 303–373 Coral Reefs of the USA. Springer.

582 Rosenberg, E., and Y. Loya. 2004. Coral health and disease. Springer.

583 Sandin, S. A., J. E. Smith, E. E. DeMartini, E. A. Dinsdale, S. D. Donner, A. M. Friedlander, T.
584 Konotchick, M. Malay, J. E. Maragos, D. Obura, and others. 2008. Baselines and
585 degradation of coral reefs in the northern Line Islands. PLoS One 3:e1548.

586 Scheffer, M., J. Bascompte, W. A. Brock, V. Brovkin, S. R. Carpenter, V. Dakos, H. Held, E. H. Van
587 Nes, M. Rietkerk, and G. Sugihara. 2009. Early-warning signals for critical transitions.
588 Nature 461:53–59.

589 Schutte, V. G. W., E. R. Selig, and J. F. Bruno. 2010. Regional spatio-temporal trends in
590 Caribbean coral reef benthic communities. Marine Ecology Progress Series 402:115–122.

591 Smith, T. B., M. E. Brandt, J. M. Calnan, R. S. Nemeth, J. Blondeau, E. Kadison, M. Taylor, and P.
592 Rothenberger. 2013. Convergent mortality responses of Caribbean coral species to
593 seawater warming. Ecosphere 4:87.

Stocker, T. F., D. Qin, G. K. Plattner, M. Tignor, S. K. Allen, J. Boschung, A. Nauels, Y. Xia, V. Bex, and P. M. Midgley. 2013. IPCC, 2013: Climate Change 2013: The Physical Science Basis. Contribution of Working Group I to the Fifth Assessment Report of the Intergovernmental Panel on Climate Change. Cambridge Univ Press, Cambridge, United Kingdom and New York, NY, USA.

Walther, G.-R., E. Post, P. Convey, A. Menzel, C. Parmesan, T. J. C. Beebee, J.-M. Fromentin, O. Hoegh-Guldberg, and F. Bairlein. 2002. Ecological responses to recent climate change. Nature 416:389–395.

Short descriptions of Ecological Archives material

Appendix A: Detailed methods

Appendix B: Mathematical proofs of equations (2) and (3)

Appendix C: Residual analysis

Appendix D: Simulation studies

Appendix E: Additional results

Figure legends

Figure 1. Average cover of scleractinian corals (solid lines) and macroalgae (broken lines) in three habitats (Tektite, Yawzi Point, and the random-sites habitat) on the south shore of St. John.

Figure 2. Cover composition of coral, macroalgae, and 'other' for three shallow habitats on the south shore of St. John. Large plus (+) symbols show the metric center (appendix A) of the quasi-stationary distribution for 2012, and are enclosed in approximate 50%, 80%, and 95% probability contours. Approximate probability contours require an assumption that $\mathbf{u}_t$ and $\mathbf{e}_t$ are normally distributed. See Appendix D for a comparison to the quasi-stationary distribution when these normality assumptions are relaxed. Small plus symbols trace how the center has changed from 1992 – 2012. Open circles show annual compositions. Data shown for the RS habitat are from site RS-15 (see map in Edmunds [2013]), which had the third greatest annual coral cover of the six sites. Other sites are shown in Fig. A1.

Figure 3. Two measures of stability of benthic communities at Tektite, Yawzi Point, and random-site (RS) habitats. (a) Coefficient of variation of coral cover in the quasi-stationary distribution. (b) Spectral radius of the matrix **B**. Larger values of the spectral radius indicate slower return to the quasi-stationary distribution following a disturbance. Error bars are ±1 robust bootstrap s.e.

Figure 4. Proportional sensitivities (i.e., $\left(d\boldsymbol{\mu}_\mathrm{p}/d\boldsymbol{\mu}_\mathrm{u}\right)\times\left(1/\boldsymbol{\mu}_\mathrm{p}\right)$) and annual trend (i.e., $\left(d\boldsymbol{\mu}_\mathrm{p}/dt^*\right)\times\left(1/\boldsymbol{\mu}_\mathrm{p}\right)$) of mean coral cover at the quasi-stationary distribution for Tektite, Yawzi Point and the random sites (RS). Sensitivities are calculated with respect to (a) a 50% increase in annual hurricane activity, (b) a 50% increase in DHM per year, and (c) the

additional annual trend, after accounting for hurricanes and sea temperature. Error bars are ±1 robust bootstrap s.e.

Figure 5. Quasi-stationary distributions of 6 coral genera found at the random sites habitat. For each genus, solid lines indicate medians, the boxes extend from the lower to the upper quartiles, and whiskers extend from the 2.5th to the 97.5th percentiles.

Figure 6. Proportional sensitivities (i.e., $\left(d\boldsymbol{\mu}_{\mathrm{p}}/d\boldsymbol{\mu}_{\mathrm{u}}\right)\times\left(1/\boldsymbol{\mu}_{\mathrm{p}}\right)$) and annual trend (i.e., $\left(d\boldsymbol{\mu}_{\mathrm{p}}/dt^{*}\right)\times\left(1/\boldsymbol{\mu}_{\mathrm{p}}\right)$) of mean coral cover for 6 coral genera found at the random sites habitat. Sensitivities are calculated with respect to (a) a 50% increase in annual hurricane activity, (b) a 50% increase in DHM per year, and (c) the additional annual trend, after accounting for hurricanes and sea temperature. Error bars are ±1 robust bootstrap s.e.

Figure 1.

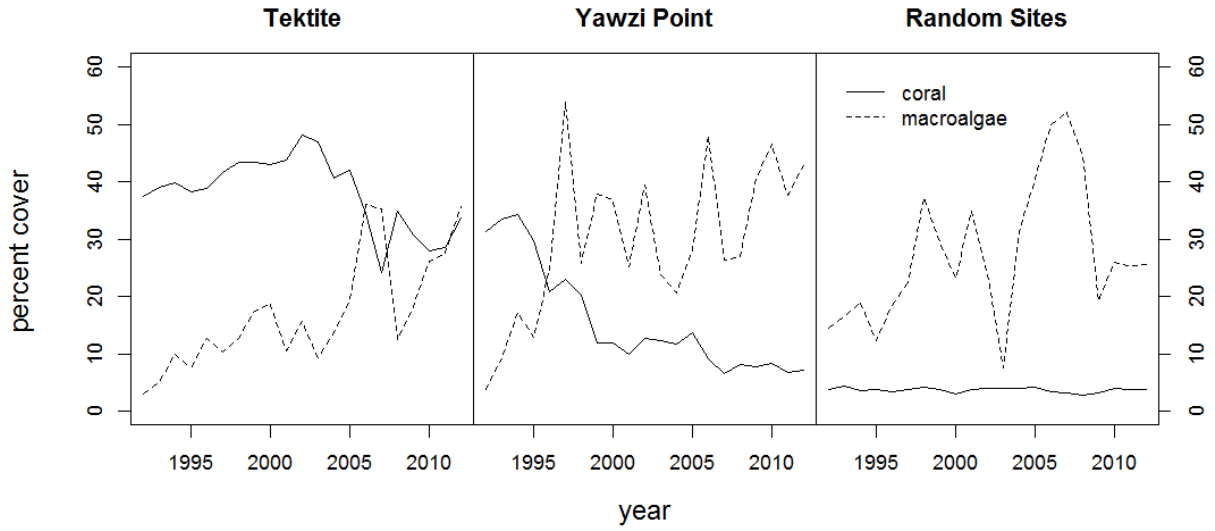
Tektite
Yawzi Point
Random Sites
coral
macroalgae
percent cover
0
10
20
30
40
50
60
1995
2000
2005
2010
year

Figure 2.

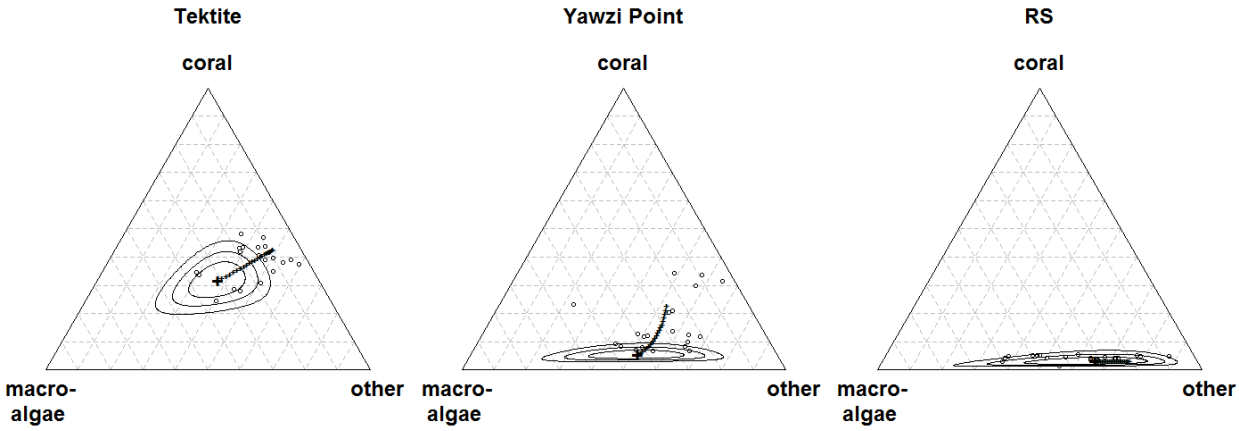
Tektite
coral
macro-
algae
other
Yawzi Point
coral
macro-
algae
other
RS
coral
macro-
algae
other

Figure 3.

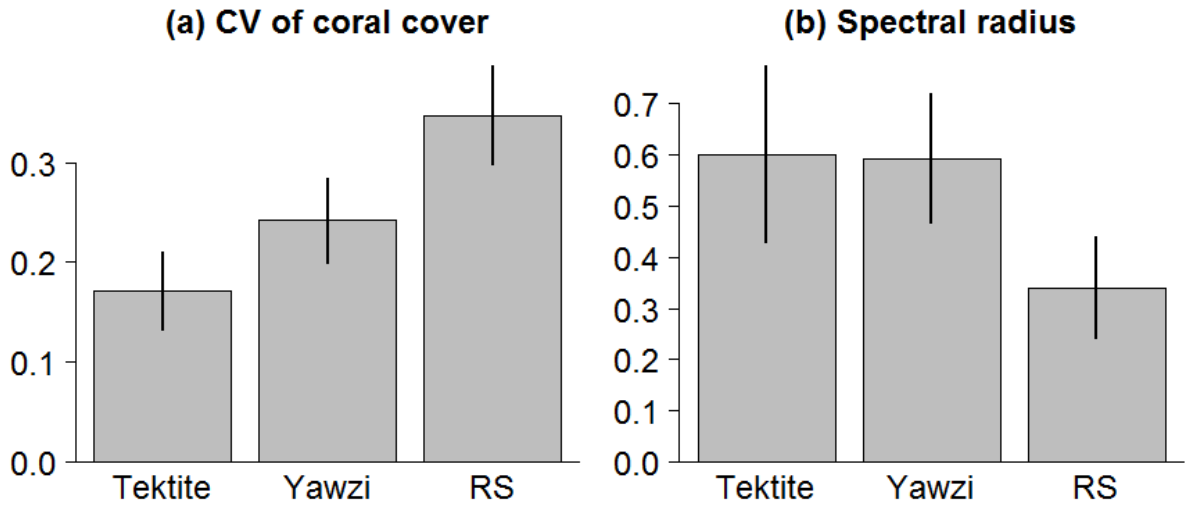
(a) CV of coral cover
0.0
0.1
0.2
0.3
Tektite
Yawzi
RS
(b) Spectral radius
0.0
0.1
0.2
0.3
0.4
0.5
0.6
0.7
Tektite
Yawzi
RS

Figure 4.

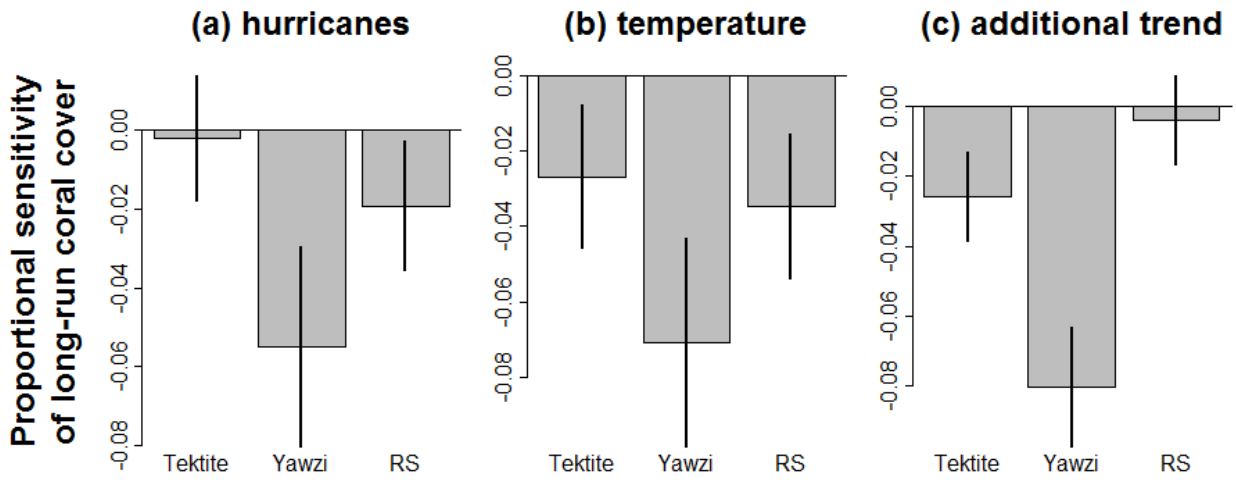
(a) hurricanes
(b) temperature
(c) additional trend
Proportional sensitivity of long-run coral cover
0.00
-0.02
-0.04
-0.06
-0.08
Tektite
Yawzi
RS

Figure 5.

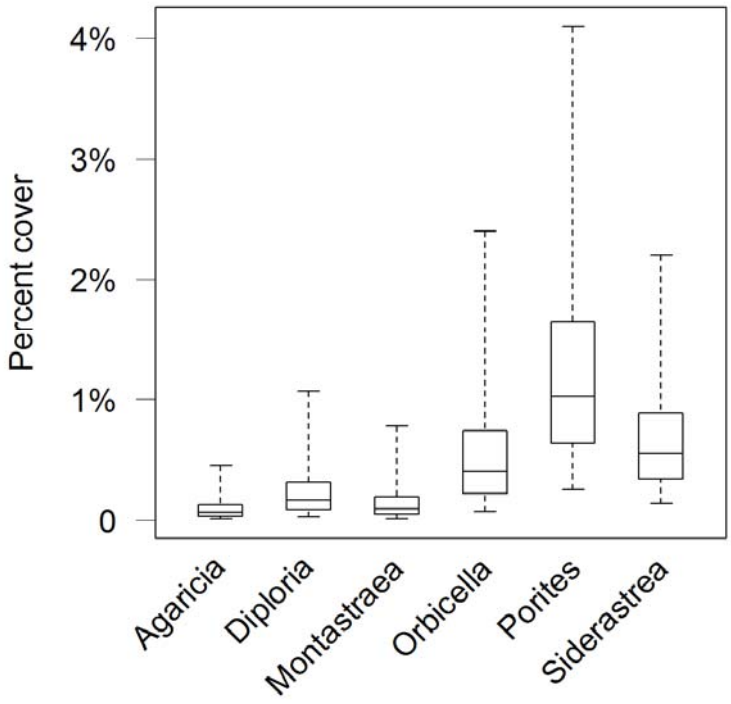
Percent cover
4%
3%
2%
1%
0
Agaricia
Diploria
Montastraea
Orbicella
Porites
Siderastrea

Figure 6.

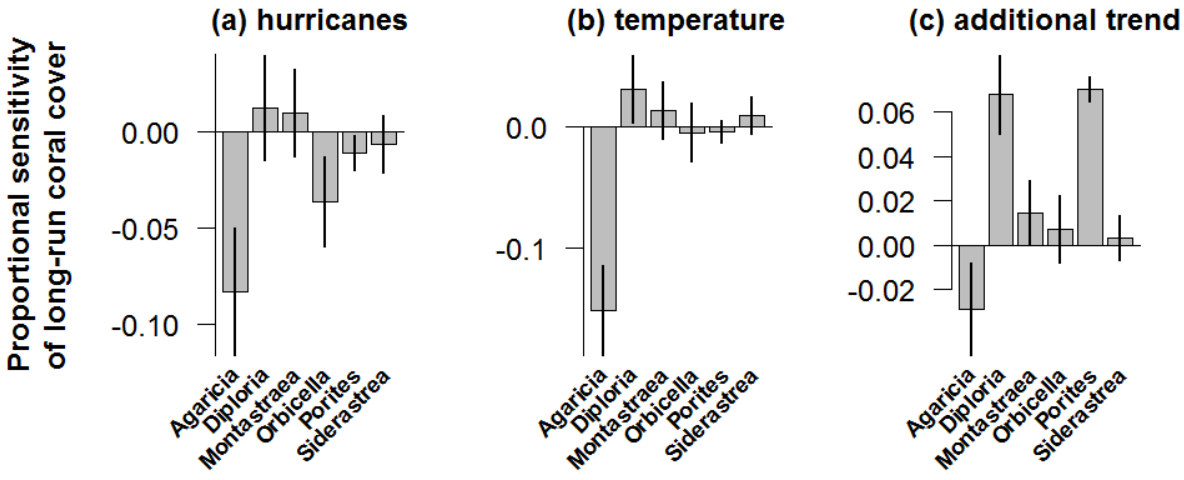
Proportional sensitivity of long-run coral cover
(a) hurricanes
(b) temperature
(c) additional trend
0.00
-0.05
-0.10
0.0
-0.1
0.06
0.04
0.02
0.00
-0.02
Agaricia
Diploria
Montastraea
Orbicella
Porites
Siderastrea

Appendices for online archives

Appendix A: Detailed methods

Data collection

Thirty photoquadrats (1 x 1 m) were recorded annually at Tektite and Yawzi Point, and 108-240 photoquadrats (0.5 x 0.5 m) were recorded at the RS (the RS sample size was increased in 2000 with the application of digital photography). Percentage cover of each group was determined using the software CPCe (Kohler & Gill 2006) with 200 randomly located dots on each image. A map of all study locations can be found in Edmunds (2013). Annual cover composition at each of the six sites that comprise the RS data are shown in Fig. A1.

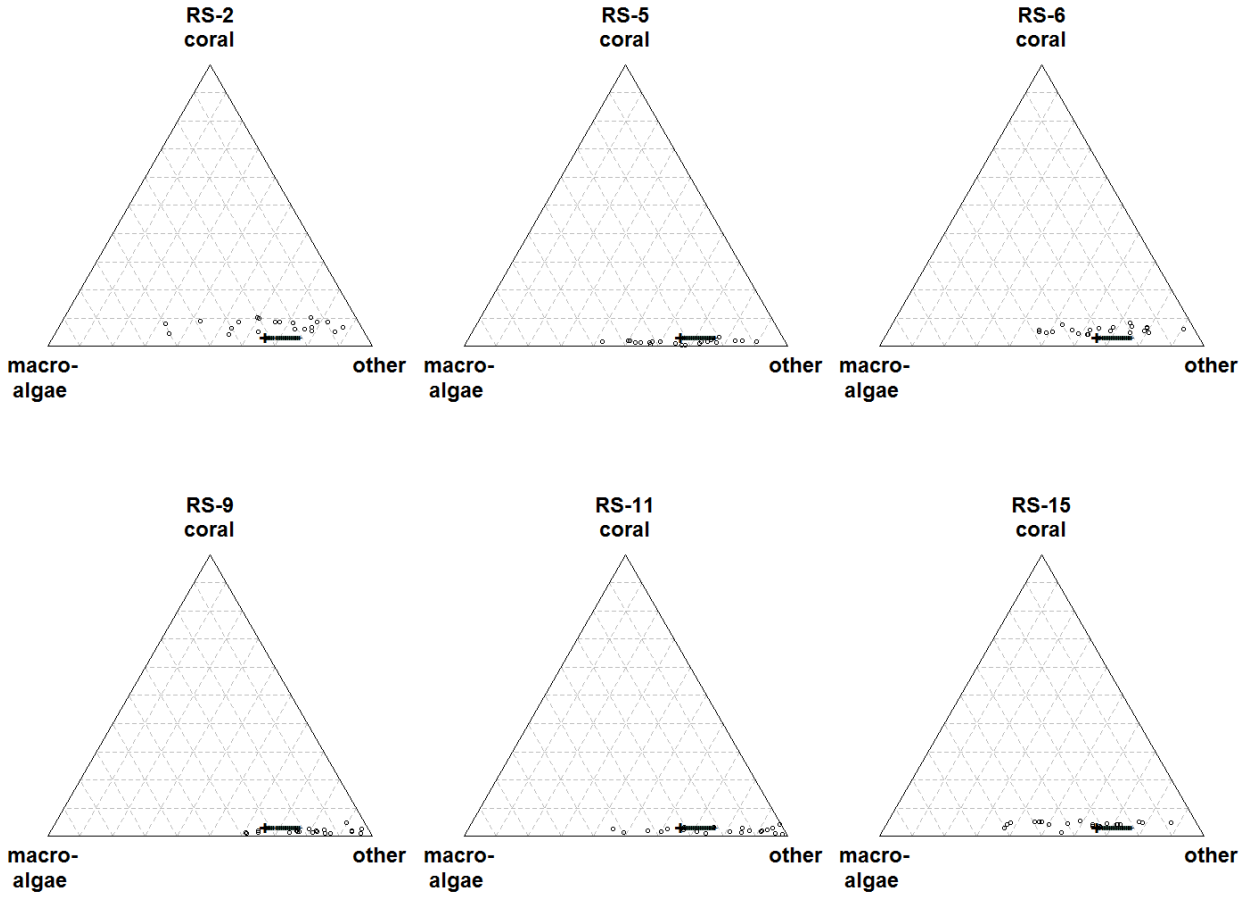

Figure A1. Composition of coral cover, macroalgal cover, and 'other' for the six sites that comprise the RS data. Site labels correspond to designations from Edmunds (2013). Large plus (+) symbols show the metric center of the quasi-stationary distribution for 2012, and small plus symbols trace how this mean has changed from 1992 – 2012. Open circles symbols show annual compositions.

Vectors and matrices in MAR model

For the cover analysis, the vectors and matrices in the MAR model (eq. 1) have the following forms:

$$\mathbf{x}_t = \begin{bmatrix} x_1 \\ x_2 \end{bmatrix}_t ; \ \mathbf{a} = \begin{bmatrix} a_1 \\ a_2 \end{bmatrix}; \ \mathbf{B} = \begin{bmatrix} b_{11} & b_{12} \\ b_{21} & b_{22} \end{bmatrix}; \ \mathbf{C} = \begin{bmatrix} c_{11} & c_{12} \\ c_{21} & c_{22} \end{bmatrix}; \ \mathbf{z} = \begin{bmatrix} z_1 \\ z_2 \end{bmatrix}; \ \mathbf{u}_t = \begin{bmatrix} u_1 \\ u_2 \end{bmatrix}_t ; \ \mathbf{e}_t = \begin{bmatrix} \varepsilon_1 \\ \varepsilon_2 \end{bmatrix}_t . \quad (6)$$

For the RS habitat, there is a unique intercept vector **a** for each of the six sites. For the taxonomic analysis, the vectors and matrices in the MAR model (eq. 1) have the following forms:

$$\mathbf{x}_t = \begin{bmatrix} x_1 \\ x_2 \\ x_3 \\ x_4 \\ x_5 \\ x_6 \end{bmatrix}_t ; \ \mathbf{a} = \begin{bmatrix} a_1 \\ a_2 \\ a_3 \\ a_4 \\ a_5 \\ a_6 \end{bmatrix}; \ \mathbf{B} = \begin{bmatrix} b_{11} & 0 & 0 & 0 & 0 & 0 \\ 0 & b_{22} & 0 & 0 & 0 & 0 \\ 0 & 0 & b_{33} & 0 & 0 & 0 \\ 0 & 0 & 0 & b_{44} & 0 & 0 \\ 0 & 0 & 0 & 0 & b_{55} & 0 \\ 0 & 0 & 0 & 0 & 0 & b_{66} \end{bmatrix}; \ \mathbf{C} = \begin{bmatrix} c_{11} & c_{12} \\ c_{21} & c_{22} \\ c_{31} & c_{32} \\ c_{41} & c_{42} \\ c_{51} & c_{52} \\ c_{61} & c_{62} \end{bmatrix};$$

$$\mathbf{z} = \begin{bmatrix} z_1 \\ z_2 \\ z_3 \\ z_4 \\ z_5 \\ z_6 \end{bmatrix}; \ \mathbf{u}_t = \begin{bmatrix} u_1 \\ u_2 \end{bmatrix}_t ; \ \mathbf{e}_t = \begin{bmatrix} \varepsilon_1 \\ \varepsilon_2 \\ \varepsilon_3 \\ \varepsilon_4 \\ \varepsilon_5 \\ \varepsilon_6 \end{bmatrix}_t . \quad (7)$$

For the RS habitat, there is a unique intercept vector **a** and a unique trend vector **z** for each of the six sites. The only parameters that are shared between the cover and taxonomic analyses are the mean vector $\boldsymbol{\mu}_u$ and variance matrix $\boldsymbol{\Sigma}_u$ for the environmental covariates. (This is because the values of the environmental covariates are the same for both cover and taxonomic analysis.) All other model parameters have separate values for the cover and taxonomic analysis.

Data transformation

In notation, if we write the proportional cover of coral, macroalgae, and 'other' as p_1, p_2, and p_3, respectively, then the corresponding isometric log-ratio (ilr) coordinates are

$$x_1 = \frac{1}{\sqrt{2}} \ln\left(\frac{p_1}{p_2}\right), \quad x_2 = \frac{2}{\sqrt{6}} \ln\left(\frac{\sqrt{p_1 p_2}}{p_3}\right) . \tag{8}$$

With a change in sign, this is the same transformation used by Cooper et al. (*in press*). In short, ilr coordinates are orthogonal contrasts of the log proportions; results on the proportion scale do not depend on the particular set of contrasts chosen. Here, x_1 quantifies the difference between coral vs. macroalgae cover, and x_2 quantifies the difference between the geometric mean of coral and macroalgae cover vs. 'other'. This particular set of contrasts is based on a sequential binary partition (Egozcue and Pawlowsky-Glahn 2011; see their formula for 'balances' in their section 2.4). As Cooper et al. (*in press*) note, an ilr transformation is a sensible transformation for community compositions, because exponential growth of all components of the composition results in linear dynamics on the ilr scale (Egozcue et al. 2003). Time series of cover composition on the ilr-transformed scale are shown in fig. A2.

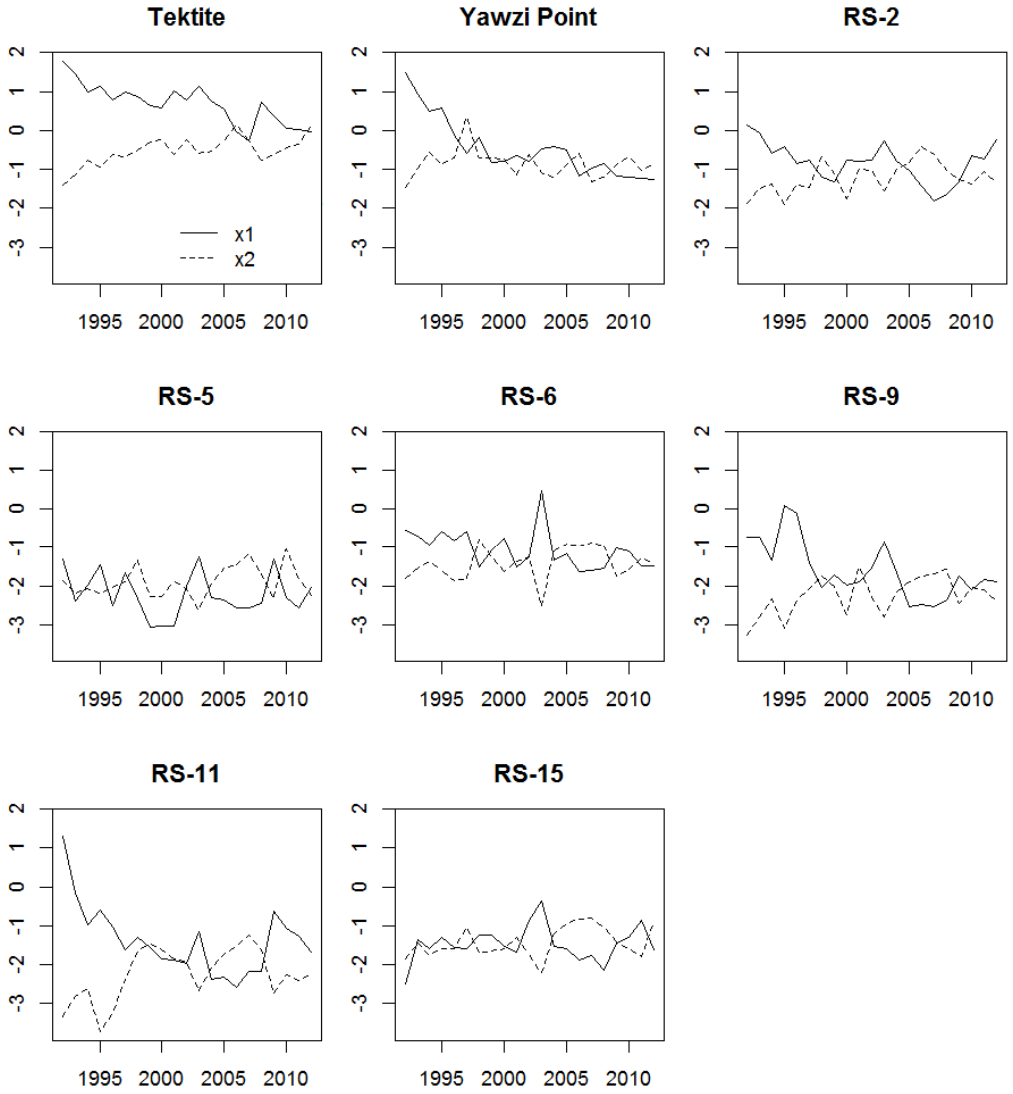

Figure A2. Cover composition in ilr coordinates for Tektite, Yawzi Point, and the 6 random sites.

To convert results back to the native proportion scale, write the cover proportions as the 3-vector **p**, write the ilr coordinates as the 2-vector **x**, and write the ilr transformation as *g*(), such that $\mathbf{x}=g(\mathbf{p})$ and $\mathbf{p}=g^{-1}(\mathbf{x})$. Applying the inverse transformation g^{-1} to $\boldsymbol{\mu}_{\mathbf{x}}$

$$\boldsymbol{\mu}_{\mathbf{p}}=g^{-1}(\boldsymbol{\mu}_{\mathbf{x}}) \tag{9}$$

yields the so-called "metric center" of the composition, which Aitchison (1989) and Pawlowsky-Glahn and Egozcue (2001) have argued provides the best measure of center for a composition. A linear approximations for the variance of the stationary distribution on the proportion scale (denoted $\mathbf{\Sigma}_p$) is simply

$$\mathbf{\Sigma}_p \approx \nabla g^{-1}(\boldsymbol{\mu}_x)\mathbf{\Sigma}_x \nabla g^{-1}(\boldsymbol{\mu}_x)^T \ . \quad (10)$$

Expressions for eq. (4)-(5) on the proportion scale follow from the chain rule of calculus:

$$\frac{d\boldsymbol{\mu}_p}{d\boldsymbol{\mu}_u} \approx \nabla g^{-1}(\boldsymbol{\mu}_x)(\mathbf{I}-\mathbf{B})^{-1}\mathbf{C}; \quad \frac{d\boldsymbol{\mu}_p}{dt^*} \approx \nabla g^{-1}(\boldsymbol{\mu}_x)(\mathbf{I}-\mathbf{B})^{-1}\mathbf{z}; \quad (11)$$

$$\frac{d\mathrm{Vec}(\mathbf{\Sigma}_p)}{d\mathrm{Vec}(\mathbf{\Sigma}_u)} \approx \left(\nabla g^{-1}(\boldsymbol{\mu}_x) \otimes \nabla g^{-1}(\boldsymbol{\mu}_x)\right)(\mathbf{I}-\mathbf{B}\otimes\mathbf{B})^{-1}(\mathbf{C}\otimes\mathbf{C}) \ . \quad (10)$$

Literature cited in Appendix A

Aitchison, J. 1989. Measures of location of compositional data sets. Mathematical Geology 21:787 – 790.

Cooper, J.K., M. Spencer, and J. F. Bruno. Stochastic dynamics of a warmer Great Barrier Reef. Ecology, *in press*.

Edmunds, P. J. 2013. Decadal-scale changes in the community structure of coral reefs of St. John, US Virgin Islands. Marine Ecology Progress Series 489:107–123.

Egozcue, J. J., and V. Pawlowsky-Glahn. 2011. Basic concepts and procedures. Pages 12–28 *in* V. Pawlowsky-Glahn and A. Buccianti, editors. Compositional data analysis: theory and applications. John Wiley and Sons New York, NY.

74 Egozcue, J. J., V. Pawlowsky-Glahn, G. Mateu-Figueras, and C. Barcelo-Vidal. 2003. Isometric
75 logratio transformations for compositional data analysis. Mathematical Geology 35:279–
76 300.
77 Kohler, K. E., and S. M. Gill. 2006. Coral Point Count with Excel extensions (CPCe): A Visual Basic
78 program for the determination of coral and substrate coverage using random point count
79 methodology. Computers & Geosciences 32:1259–1269.

80 Pawlowsky-Glahn, V., and J. J. Egozcue. 2001. Geometric approach to statistical analysis on the
81 simplex. Stochastic Environmental Research and Risk Assessment 15:384–398.

82

Appendix B: Mathematical proofs of equations (2) and (3)

Fix time *t* at t^*. Re-write eq. (1) as

$$\mathbf{x}_t = \mathbf{a} + \mathbf{z}t^* + \mathbf{C}\boldsymbol{\mu}_\mathbf{u} + \mathbf{B}\mathbf{x}_{t-1} + \mathbf{C}\mathbf{u}_t - \mathbf{C}\boldsymbol{\mu}_\mathbf{u} + \mathbf{e}_t \qquad t = 2,3,....$$

Set the constant $\mathbf{a} + \mathbf{z}t^* + \mathbf{C}\boldsymbol{\mu}_\mathbf{u}$ equal to $\tilde{\mathbf{a}}$, and set the random sum $\mathbf{C}\mathbf{u}_t - \mathbf{C}\boldsymbol{\mu}_\mathbf{u} + \mathbf{e}_t$ equal to $\tilde{\mathbf{e}}$. Note that the expectation of $\tilde{\mathbf{e}}$ is $\mathrm{E}\left[\mathbf{C}\mathbf{u}_t - \mathbf{C}\boldsymbol{\mu}_\mathbf{u} + \mathbf{e}_t\right] = \mathbf{C}\boldsymbol{\mu}_\mathbf{u} - \mathbf{C}\boldsymbol{\mu}_\mathbf{u} = \mathbf{0}$, and the variance of $\tilde{\mathbf{e}}$ is $\mathrm{Var}\left[\mathbf{C}\mathbf{u}_t - \mathbf{C}\boldsymbol{\mu}_\mathbf{u} + \mathbf{e}_t\right] = \mathbf{C}\boldsymbol{\Sigma}_\mathbf{u}\mathbf{C}^T + \boldsymbol{\Sigma}_\mathbf{e}$ (recall that $\mathbf{u}_t$ and $\mathbf{e}_t$ are assumed independent). Thus, eq. (1) can be re-written as

$$\mathbf{x}_t = \tilde{\mathbf{a}} + \mathbf{B}\mathbf{x}_{t-1} + \tilde{\mathbf{e}}_t \qquad t = 2,3,....$$

which is the multivariate AR(1) model from Ives et al. (2003) (their eq. 10). Thus, the mean and variance of the stationary distribution follow immediately as

$$\begin{aligned}\boldsymbol{\mu}_\mathbf{x} &= \left(\mathbf{I} - \mathbf{B}\right)^{-1}\tilde{\mathbf{a}} \\ &= \left(\mathbf{I} - \mathbf{B}\right)^{-1}\left(\mathbf{a} + \mathbf{C}\boldsymbol{\mu}_\mathbf{u} + \mathbf{z}t^*\right)\end{aligned}$$

and

$$\begin{aligned}\mathrm{Vec}\left(\boldsymbol{\Sigma}_\mathbf{x}\right) &= \left(\mathbf{I} - \mathbf{B}\otimes\mathbf{B}\right)^{-1}\mathrm{Vec}\left(\mathrm{Var}\left(\tilde{\mathbf{e}}\right)\right) \\ &= \left(\mathbf{I} - \mathbf{B}\otimes\mathbf{B}\right)^{-1}\mathrm{Vec}\left(\mathbf{C}\boldsymbol{\Sigma}_\mathbf{u}\mathbf{C}^T + \boldsymbol{\Sigma}_\mathbf{e}\right).\end{aligned}$$

Appendix C: Residual analysis

The figures in this appendix show diagnostic plots for residuals from the cover analysis (Figs. C1 – C2) and the taxonomic analysis (Figs. C3 – C4). The MAR model assumes that the vector-valued residuals are serially independent and identically distributed. Thus, residual plots such as these are useful for diagnosing whether or not the variance of the residuals changes with time, or is different for large or small fitted values.

Few features stand out in the residual plot for the cover analysis, except for perhaps the occasional residual with a very large absolute value. Residuals from the taxonomic analysis seem do occasionally demonstrate banding characteristic of log-transformed data for that is below the limit of detection. For example, *Montastrea* was not observed at site RS-5 for 1992 – 2004, and was only detected at small densities in three of the years thereafter. Such banding suggests that, for those coral genera that were frequently below the detection limit from one or more sites (namely, *Montastrea*), sensitivities to hurricanes and sea temperature may be near zero simply because environment will have no observed impact on the growth rates of an undetected coral.

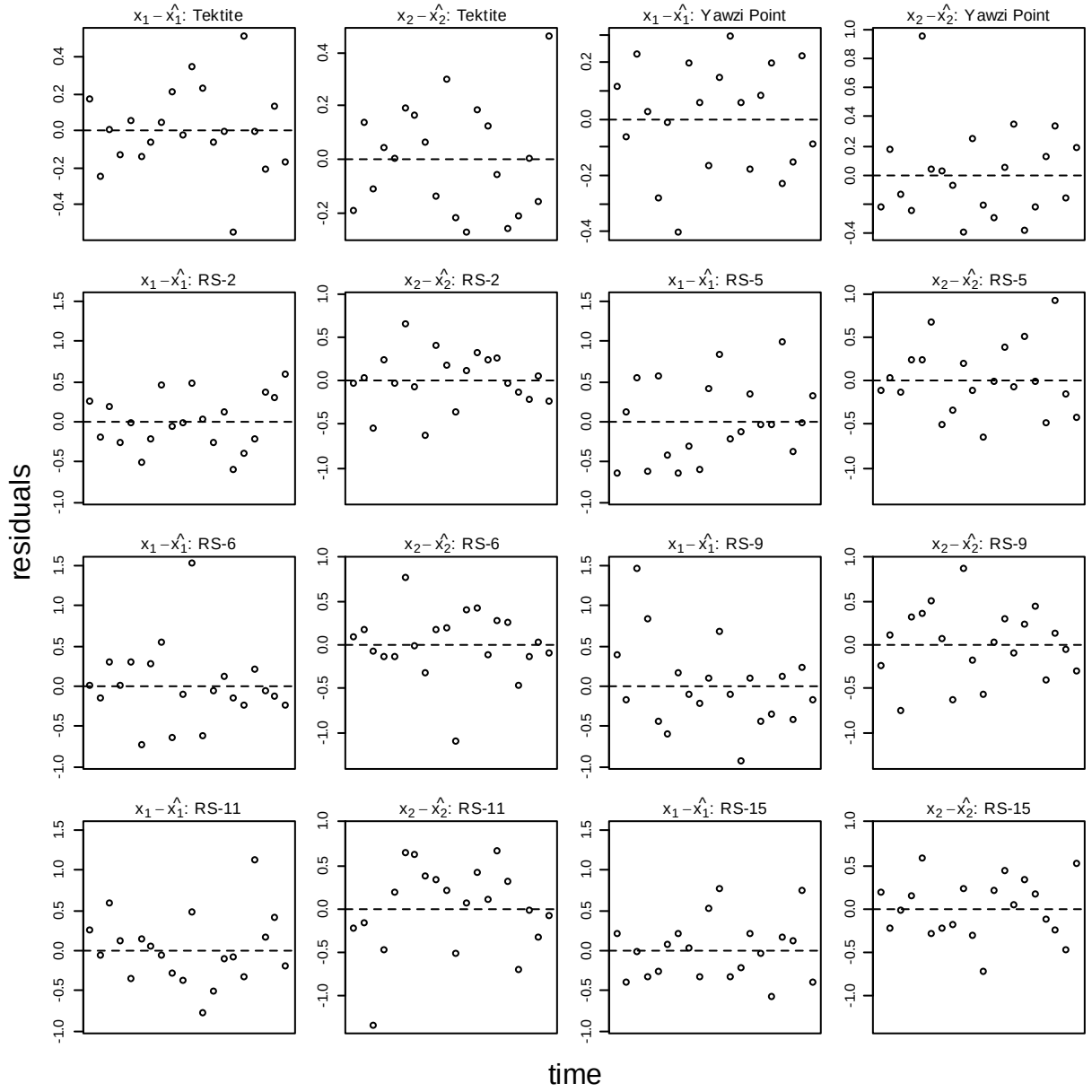

Figure C1. Plots of residuals vs. time for ilr-transformed compositions at Tektite, Yawzi Point, and the random sites.

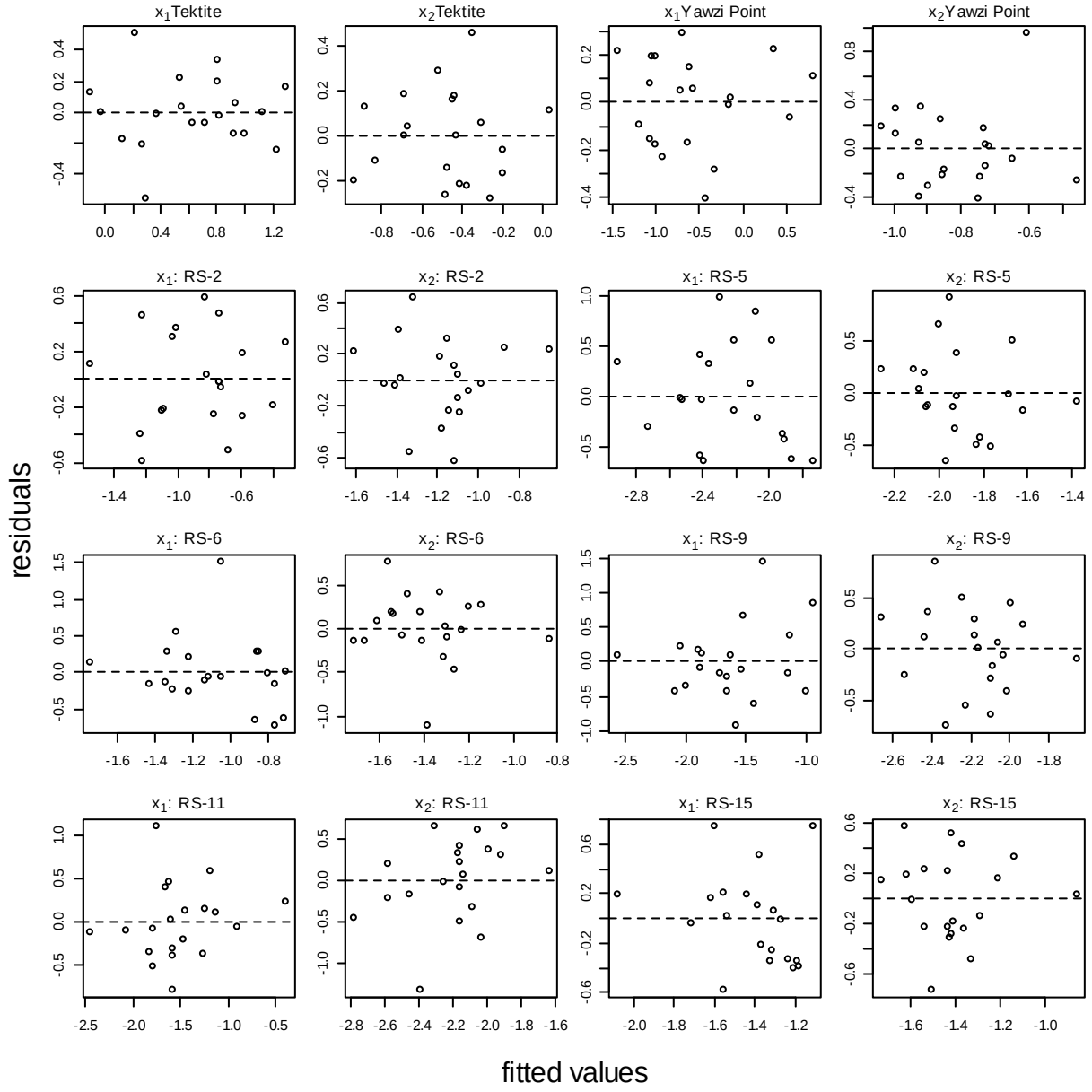

Figure C2. Plots of residuals vs. fitted values for ilr-transformed compositions at Tektite, Yawzi Point, and the individual random sites.

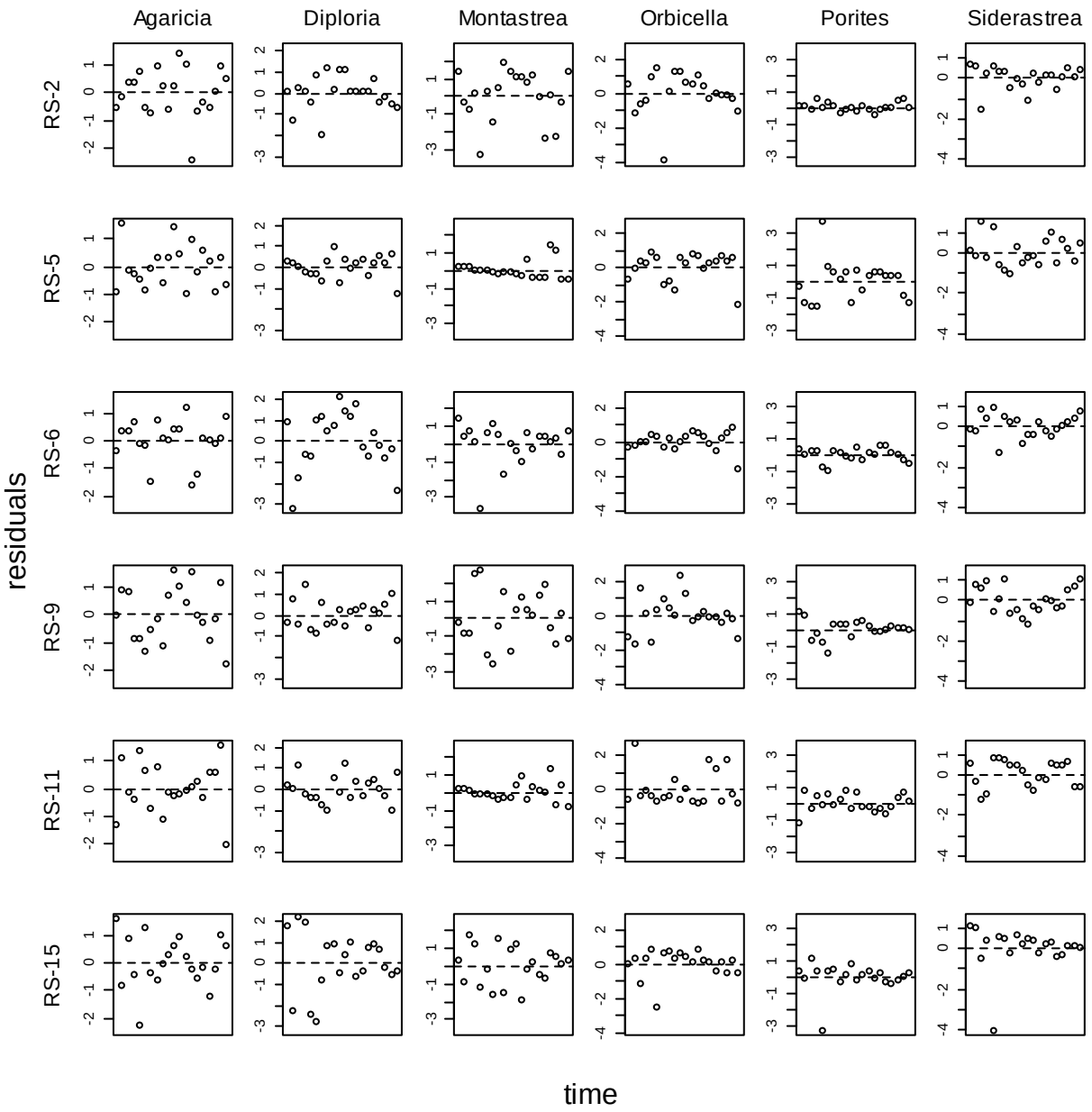

Figure C3. Plots of residuals vs. time for coral genera at individual random sites.

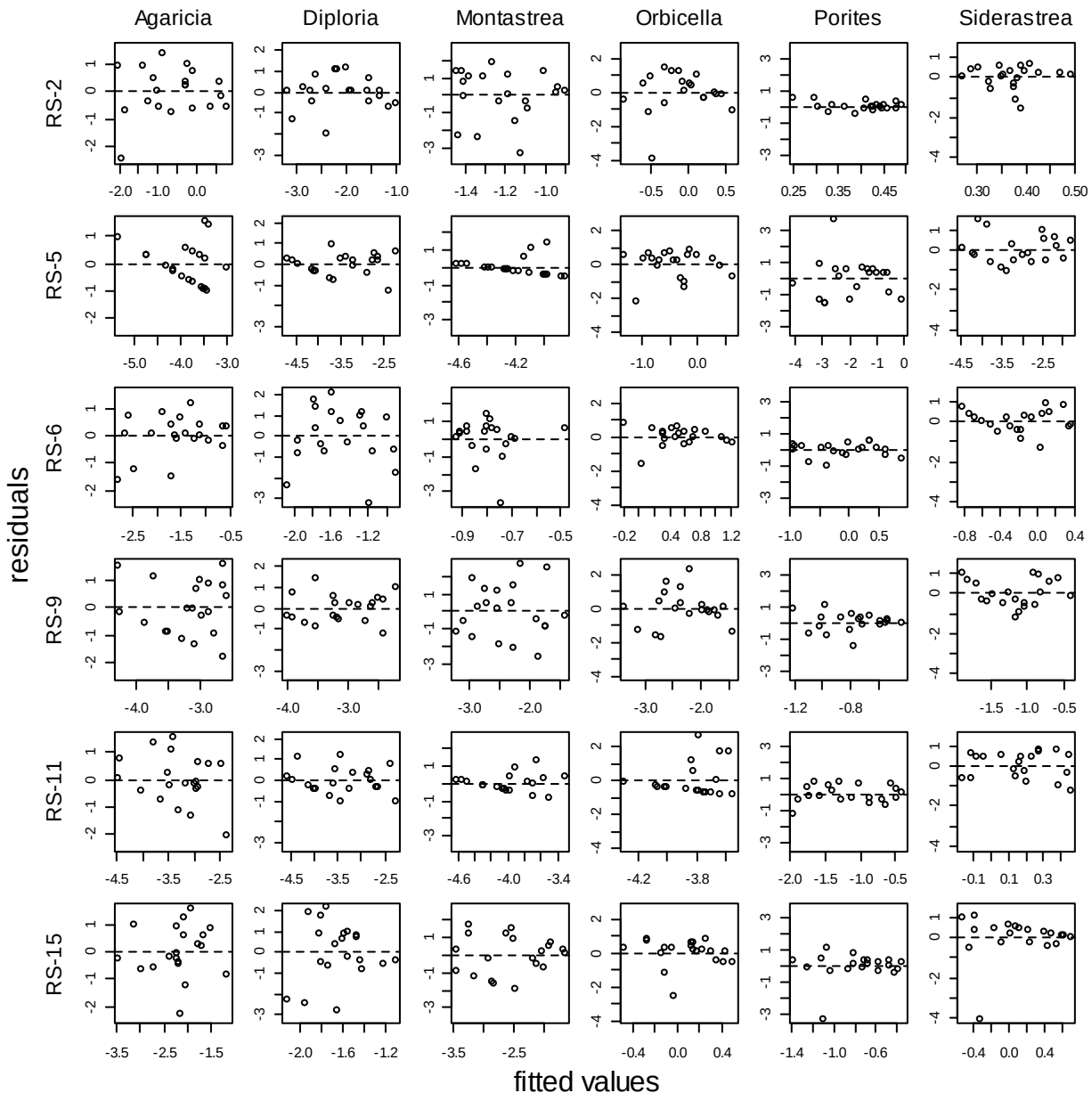

121

122 *Figure C4. Plots of residuals vs. fitted values for coral genera at individual random sites.*

123

Appendix D: Simulation studies

Simulation study 1: Sampling distributions of MAR model parameters and stability metrics under different magnitudes of trend

We conducted a small simulation study to investigate whether the trend covariate in eq. (1) impacted the estimation of several of the stability metrics calculated in the cover analysis. For each of the three habitats, we simulated data sets using the estimated values of **a**, **B**, and **C** in eq. (1) as the generative model. For the RS habitat, we used the average estimate of **a** across all sites. We simulated environmental variation and residual variation by sampling with replacement from the observed environmental vectors and the estimated residual vectors, respectively. Because our simulation focused on the effect of time, we ran simulations where **z** in the generative model equaled $k\mathbf{z}$, where k is a multiplier that diminished or amplified the trend by a factor of k=0, 0.5, 1, 1.5 or 2, and **z** equaled its estimated value. We refer to the k as the "trend multiplier". Initial values for the cover composition were drawn from the estimated quasi-stationary distribution for the first year of our study. Thus, we had 15 total simulation scenarios (three habitats crossed with five values of k). We simulated 1000 data sets for each simulation scenario, with each data set lasting for 21 time steps (the same duration as the actual data). Rare simulations that generated an estimated **B** matrix with a spectral radius greater than 1 were discarded. We report the mean, interquartile range, and 10^{th} and 90^{th} percentiles of the empirical sampling distribution for several model parameters and derived stability metrics.

Figure D1 shows the empirical sampling distribution for the elements of **a**, **B**, **C**, and **z** for each habitat and each value of *k*, along with actual values from the generative models. Not surprisingly, estimators are biased. This bias is not surprising because it is known that the conditional least-squares estimators of autoregressive models are only asymptotically unbiased, and will be biased for short time series. The key feature of figure D1, however, is that the marginal sampling distribution of the elements of **a**, **B**, and **C** do not appear to depend on the value of *k*. The standard error of the elements of **z** increases as *k* increases, but any bias in the elements of **z** appears to be small.

Figure D2 shows the empirical sampling distribution of several derived metrics for the same simulation scenarios. Results suggest varying degrees of bias in derived quantities, although the magnitude of the bias only depends minimally on the strength of the trend. Means of the quasi-stationary distribution — either on the ilr-transformed scale or on the proportion scale — show negligible bias. The CV of proportional coral cover at the quasi-stationary distribution is slightly downwardly biased for the Tektite scenario, and slightly upwardly biased for the RS. Sensitivities of mean coral cover (again, on the proportion scale) to both environmental covariates and the trend all seem to be estimated with little or negligible bias.

The spectral radius of the **B** matrix is biased for all simulation scenarios for Tektite and Yawzi Point, and in these cases is negatively biased (that is, the true spectral radius is larger than the average estimated spectral radius). That the spectral radius is estimated with bias is perhaps not surprising, given the strong non-linearity inherent in calculating eigenvalues.

Nevertheless, the bias makes it clear that differences between spectral radii across habitats (fig. 2b of the main text) should be interpreted cautiously.

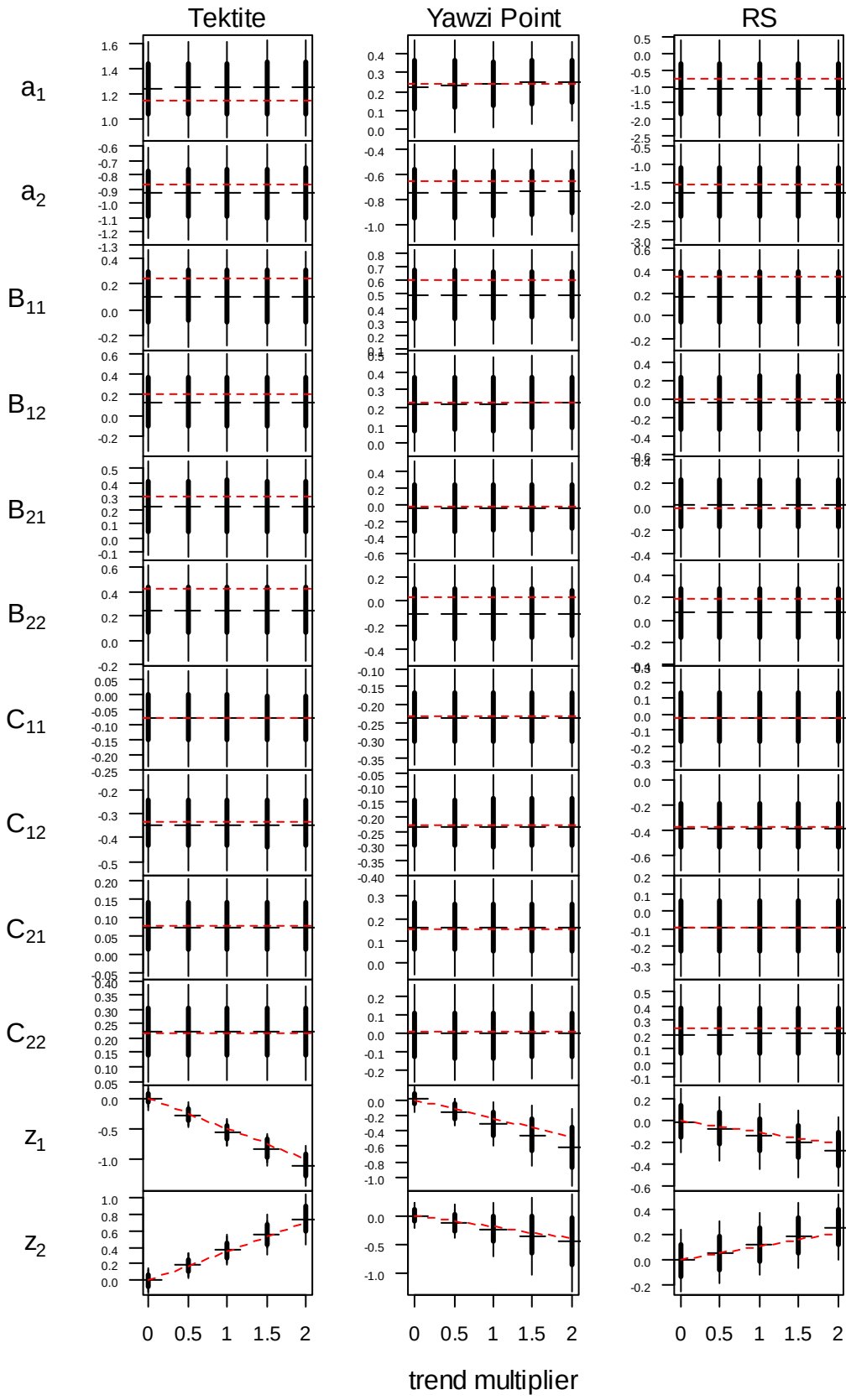
Tektite
Yawzi Point
RS
a_1
a_2
B_{11}
B_{12}
B_{21}
B_{22}
C_{11}
C_{12}
C_{21}
C_{22}
z_1
z_2
0 0.5 1 1.5 2
trend multiplier

*Figure D1 (previous page). Sampling distributions of the elements of **a**, **B**, **C**, and **z** for different simulated scenarios. Columns of panels correspond to the habitat that was used as the generative model, rows of panels show different parameters, and segments within panels show different values of the trend multiplier. Horizontal hashes show the average parameter estimate, thick vertical line segments span the interquartile range of the sampling distribution, and thin vertical line segments range from the 10^{th} percentile to the 90^{th} percentile of the sampling distribution. Red lines connect actual parameter values from the generative model.*

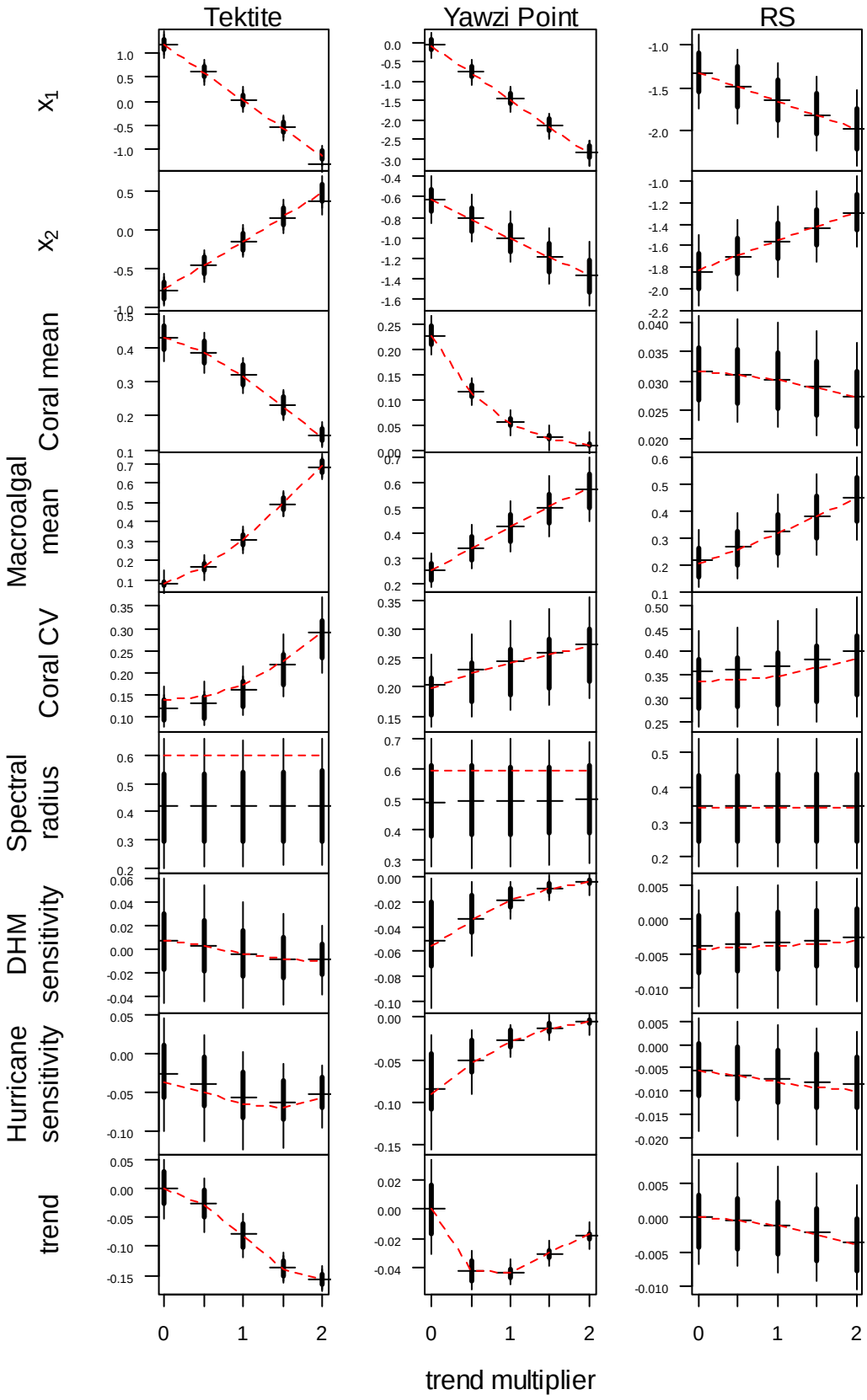
Tektite
Yawzi Point
RS
x_1
x_2
Coral mean
Macroalgal mean
Coral CV
Spectral radius
DHM sensitivity
Hurricane sensitivity
trend
trend multiplier

Figure D2 (previous page). Sampling distributions of derived quantities of interest for different simulated scenarios. Basic arrangement of panels is the same as Figure D1. First two rows: elements of $\boldsymbol{\mu}_x$ *(quasi-stationary distribution on the ilr-transformed scale). Third and fourth rows: elements of* $\boldsymbol{\mu}_p$ *, mean coral and macroalgal cover at the quasi-stationary distribution on the proportion scale. Fifth row: CV of coral cover at the quasi-stationary distribution, on the proportion scale. Sixth row: spectral radius. Seventh and eight rows: Sensitivity of average coral cover to environmental covariates, on the proportion scale (*$d\boldsymbol{\mu}_p / d\boldsymbol{\mu}_u \times \left(1/\boldsymbol{\mu}_p\right)$*). Ninth row: Trend of average coral cover per year, on the proportion scale (*$d\boldsymbol{\mu}_p / dt^* \times \left(1/\boldsymbol{\mu}_p\right)$*).*

Simulation study 2: Quality of approximate probability contours in figure 2 when $\boldsymbol{u}_t$ *and* $\boldsymbol{e}_t$ *are not normally distributed.*

Neither the MAR model (eq. 1) nor any of our results (eqq. 2 – 5) require a normality assumption for either the environmental covariates in $\mathbf{u}_t$ or the random errors in $\mathbf{e}_t$. However, the approximate probability contours for the quasi-stationary distribution shown in Fig. 2 are based on the assumption that the quasi-stationary distribution is multivariate normal on the ilr-transformed scale, which in turn relies on a normality assumption for both $\mathbf{u}_t$ and $\mathbf{e}_t$. To assess the accuracy of the approximate probability contours when $\mathbf{u}_t$ and $\mathbf{e}_t$ are not normally distributed, we simulated 5000 years of dynamics for the Tektite and Yawzi Point habitat from eq. (1), fixing the trend covariate at its 2012 value, and drawing $\mathbf{u}_t$ from its observed distribution and independently drawing $\mathbf{e}_t$ from the estimated residuals from each model.

Simulations were initiated from the estimated metric center of each quasi-stationary distribution, and the first 100 years of dynamics were discarded as a burn-in. Both $\mathbf{u}_t$ and $\mathbf{e}_t$ were sampled as vectors, thus preserving correlations between environmental covariates, and between the residuals in $\mathbf{e}_t$. These simulated dynamics provide a visualization of the exact quasi-stationary distribution for these two habitats, assuming that the actual distributions of $\mathbf{u}_t$ and $\mathbf{e}_t$ are identical to their empirical distributions (Fig. D3). The proportion of simulated data points that fall within the 50%, 80% and 95% probability contours shown in Fig. 1 of the main text are: 55.9%, 82.5%, and 95.2%, respectively, for Tektite; 57.3%, 87.2% and 94.0%, respectively, for Yawzi Point; and 56.4%, 81.5% and 93.2%, respectively, for the RS . Figure D4 shows a quantile-quantile plot of the Mahalanobis distances for the simulated dynamics on the ilr-transformed scale vs. theoretical quantiles from a χ^2_2 distribution. (This plot is the multivariate analog of the familiar normal probability plot used in residual analysis.)

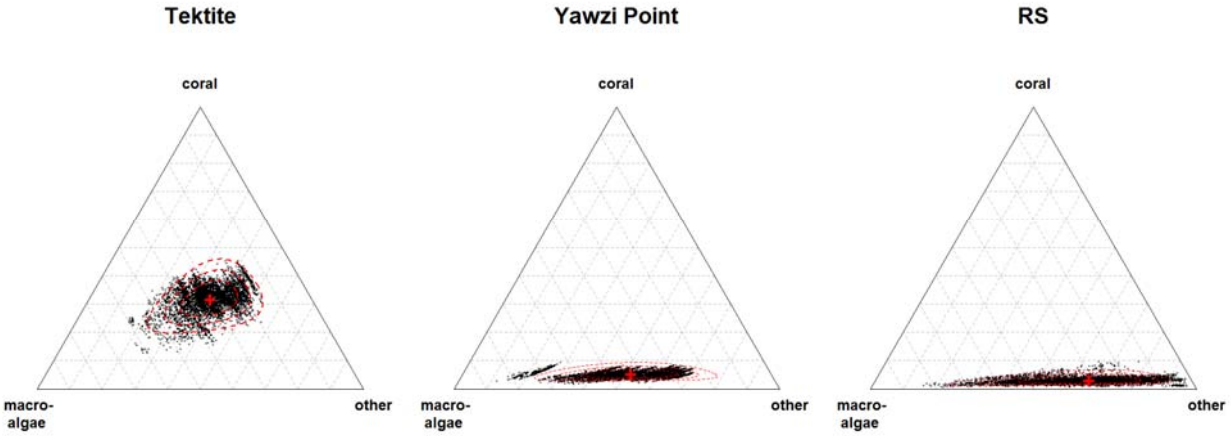

Figure D3. Triangle plots of 5000 years of simulated data from each of the three habitats, using the 2012 value of the trend covariate and the empirical distributions of $\mathbf{u}_t$ and $\mathbf{e}_t$. Red

dashed lines show approximate 50%, 80% and 95% probability contours for comparison, and are identical to those shown in Figure 1 of the main text.

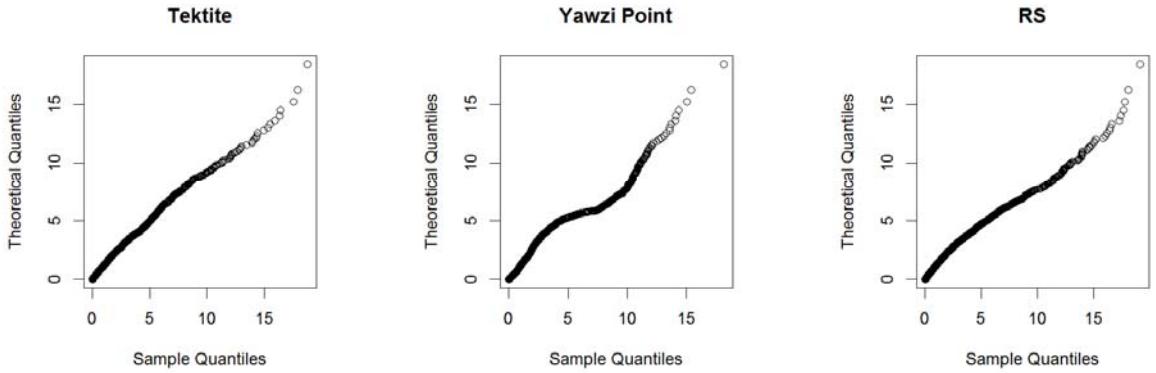

Figure D4. Quantile-quantile plots of the Mahalanobis distances of the simulated compositions (on the ilr-transformed scale) from the metric center of the quasi-stationary distribution for all three habitats, using a χ_2^2 *distribution for comparison. Departures from linearity suggest differences between the quasi-stationary distributions generated using empirical distributions of* $\boldsymbol{u}_t$ *and* $\boldsymbol{e}_t$ *(on the ilr-transformed scale) and their multivariate normal approximations.*

Taken together, these plots suggest that the approximate probability contours shown in Fig. 2 of the main text are reasonable approximations. There is some multimodality apparent in the distribution of simulated data at the Yawzi Point habitat, but this is likely a consequence of an anomalous residual (see Figure C1 of appendix C). This and other fine structure apparent in the empirical distribution of residuals is likely a consequence of the coarseness in the empirical distributions of $\mathbf{u}_t$ and $\mathbf{e}_t$ that arises from having a limited number of data points. It is unlikely that this coarseness would persist if more data were available. Thus, it seems appropriate to

233 view the normal-based probability contours as an approximation that captures the main

234 features of the quasi-stationary distribution without over-fitting to idiosyncratic fine structure.

235

Appendix E: Additional results

Tables E1 and E2 provide parameter estimates and robust bootstrap standard errors for the MAR parameters of the cover and taxonomic analysis, respectively. Parameter notation follows the detailed presentation in appendix A.

Table E1. Parameter estimates ± robust bootstrap standard errors for the cover analysis.

Parameter	Tektite	Yawzi Point	RS
a_1	0.65 ± 0.16	0.00 ± 0.25	-0.89 ± 0.50†
a_2	-0.52 ± 0.15	-0.85 ± 0.38	-1.42 ± 0.45†
b_{11}	0.25 ± 0.30	0.60 ± 0.19	0.34 ± 0.13
b_{12}	0.21 ± 0.29	0.22 ± 0.31	-0.01 ± 0.12
b_{21}	0.30 ± 0.36	-0.02 ± 0.20	-0.01 ± 0.19
b_{22}	0.43 ± 0.31	0.04 ± 0.30	0.19 ± 0.17
c_{11}	-0.08 ± 0.11	-0.23 ± 0.09	-0.03 ± 0.15
c_{12}	-0.34 ± 0.09	-0.23 ± 0.15	-0.38 ± 0.14
c_{21}	0.08 ± 0.13	0.15 ± 0.10	-0.09 ± 0.17
c_{22}	0.22 ± 0.10	0.01 ± 0.17	0.25 ± 0.16
z_1	-0.050 ± 0.019	-0.024 ± 0.024	-0.011 ± 0.016
z_2	0.035 ± 0.017	-0.020 ± 0.041	0.011 ± 0.015
σ^2_{11}	0.053 ± 0.015	0.037 ± 0.008	0.195 ± 0.043
σ^2_{12}	-0.026 ± 0.008	-0.043 ± 0.012	-0.110 ± 0.032

σ^2_{22}	0.041 ± 0.010	0.103 ± 0.034	0.152 ± 0.034

†average of site-specific values

Table E2. Parameter estimates ± robust bootstrap standard errors for the taxonomic analysis.

Parameter†	Estimate ± rbse
a_1	-1.61 ± 0.29‡
a_2	-2.78 ± 0.33‡
a_3	-2.78 ± 0.32‡
a_4	-0.98 ± 0.16‡
a_5	-0.75 ± 0.11‡
a_6	-0.68 ± 0.10‡
b_{11}	0.19 ± 0.10
b_{22}	-0.08 ± 0.12
b_{33}	-0.09 ± 0.11
b_{44}	-0.09 ± 0.10
b_{55}	-0.15 ± 0.12
b_{66}	-0.06 ± 0.10
c_{11}	-0.45 ± 0.19
c_{12}	-0.93 ± 0.21
c_{21}	0.09 ± 0.18
c_{22}	0.26 ± 0.18

c_{31}	0.07 ± 0.07
c_{32}	0.11 ± 0.11
c_{41}	-0.27 ± 0.22
c_{42}	-0.04 ± 0.25
c_{51}	-0.08 ± 0.21
c_{52}	-0.03 ± 0.21
c_{61}	-0.05 ± 0.08
c_{62}	0.08 ± 0.13
z_1	-0.023 ± 0.019‡
z_2	0.073 ± 0.023‡
z_3	0.016 ± 0.018‡
z_4	0.008 ± 0.018‡
z_5	0.081 ± 0.011‡
z_6	0.003 ± 0.011‡
σ^2_{11}	0.718 ± 0.101
σ^2_{12}	0.053 ± 0.066
σ^2_{13}	0.013 ± 0.068
σ^2_{14}	0.066 ± 0.064
σ^2_{15}	0.112 ± 0.056
σ^2_{16}	0.068 ± 0.080

σ^2_{22}	0.897 ± 0.147
σ^2_{23}	0.175 ± 0.087
σ^2_{24}	0.202 ± 0.104
σ^2_{25}	0.103 ± 0.065
σ^2_{26}	-0.025 ± 0.090
σ^2_{33}	1.153 ± 0.230
σ^2_{34}	-0.032 ± 0.088
σ^2_{35}	0.074 ± 0.051
σ^2_{36}	-0.072 ± 0.053
σ^2_{44}	0.805 ± 0.151
σ^2_{45}	-0.020 ± 0.043
σ^2_{46}	-0.057 ± 0.053
σ^2_{55}	0.489 ± 0.168
σ^2_{56}	0.145 ± 0.123
σ^2_{66}	0.499 ± 0.141

† throughout, coral genera are coded as follows: 1: *Agarcia*, 2: *Diploria*, 3: *Montastrea*, 4: *Orbicella*, 5: *Porites*, 6: *Siderastrea*

‡ average of site-specific values

Sensitivities of long-run average cover with respect to each of the environmental factors are shown in Fig. E1. (Note that the sensitivities and trend shown in Fig. E1 are absolute sensitivities, and not proportional sensitivities as reported in the main text.) The figure shows that changes in each of the environmental factors (either an increase in average hurricane activity or seawater temperature, or the annual trend after accounting for hurricanes and sea temperature) would lead to an increase in macroalgal cover at the expense of both coral and "other" at both Tektite and Yawzi Point (although the effect of hurricanes on cover composition at Tektite appears to be minimal). At the RS, increases in average seawater temperature would decrease both macroalgal and coral cover.

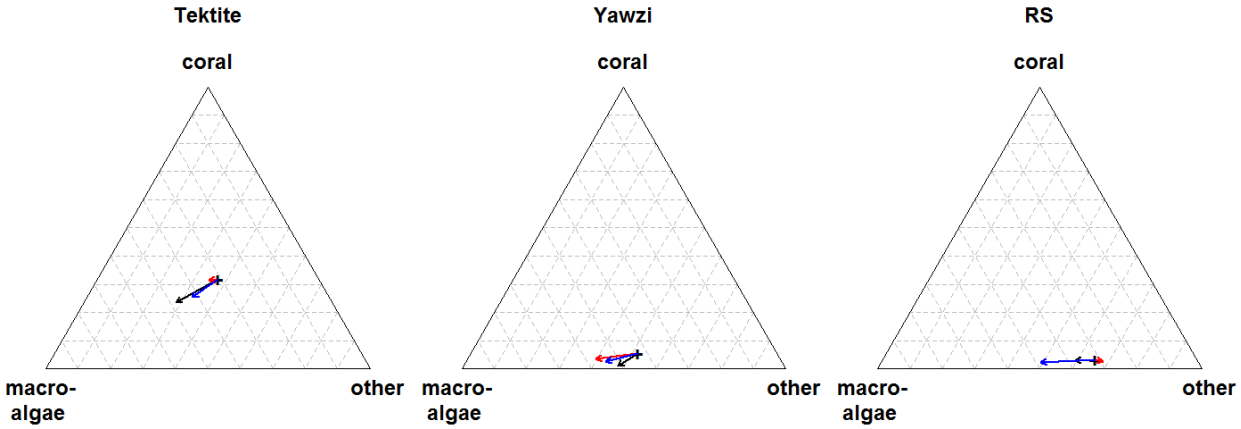

Figure E1. Sensitivity (i.e., $d\boldsymbol{\mu}_p / d\boldsymbol{\mu}_u$) and trend (i.e., $d\boldsymbol{\mu}_p / dt^*$) of the entire cover composition at three habitats. In each panel, the plus sign denotes the metric center of the 2012 quasi-stationary distribution. Red, blue and black arrows show sensitivity of cover composition with respect to hurricane activity, seawater temperature, and the annual trend respectively. To make arrows more visible, the length of each arrow corresponds to the rate of change of

the cover calculated with respect to 1 additional hurricane per year, 1 additional DHM per year, or to 10 additional years.

Sensitivities of the SD of coral cover to the SD of each of the random environmental factors are shown in Figure E2. Sensitivities are calculated assuming that the (product-moment) correlation between hurricane activity and DHMs remains fixed. That is, an increase in the SD of one environmental factor also increases the covariance between the two random environmental factors. Error bars in fig. E2 are ±1 robust bootstrap s.e. However, in most cases the bootstrap sampling distributions are severely right skewed, such that a bootstrap-based confidence interval would not be symmetric around the point estimate. For reference, the SD of hurricane activity for 1992 – 2012 was 0.55, and the SD of DHM was 0.46.

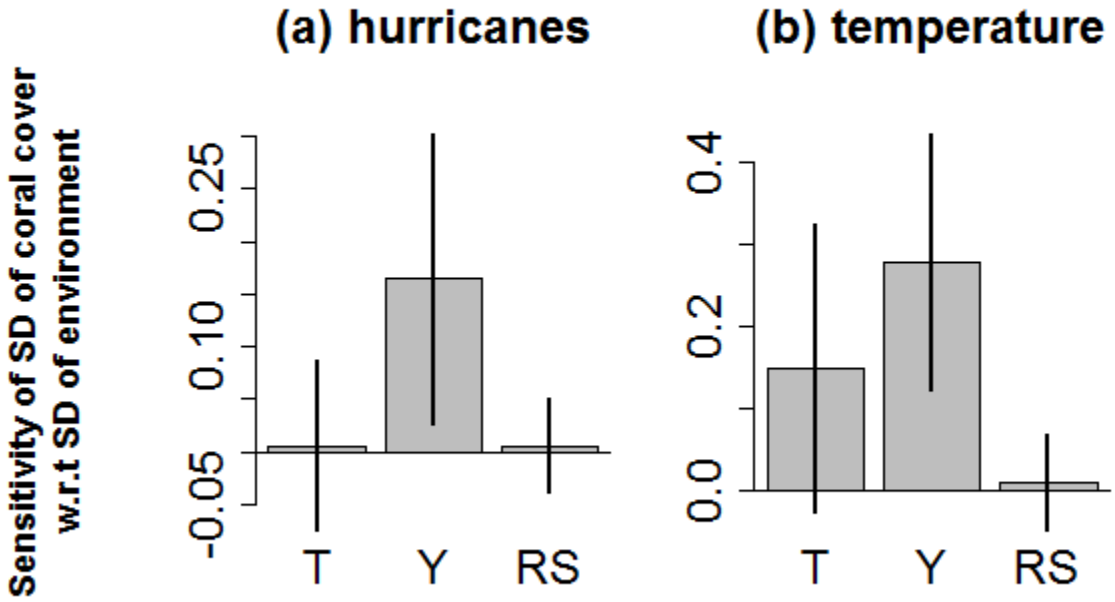

Figure E2. Sensitivity (i.e., $d\sigma_{\mathbf{p}}/d\sigma_{\mathbf{u}}$) of the SD of long-run coral cover with respect to the SD of (a) annual hurricane activity and (b) annual DHM at Tektite (T), Yawzi Point. (Y), and the random sites (RS). Sensitivities are calculated with respect to a 100% increase in the SD of the environmental covariate. Error bars are ±1 robust bootstrap s.e.